
# Data Analysis and Management track

## 65 abstracts: 17 oral and 48 posters

Irène Buvat

Laboratoire d'Imagerie Translationnelle en Oncologie, Inserm, Institut Curie, Orsay, France

irene.buvat@curie.fr

@IreneBuvat

June 11-14
2022
SNMMI ANNUAL MEETING
Vancouver, British Columbia, Canada

# Brain

Presentation #2432, SS41
Tue, June 14 3:36-3:48 114/115

# Noninvasive quantification of $^{18}$F-SynVesT-1 binding using simplified reference tissue model 2

Mika Naganawa, Jean-Dominique Gallezot, Songye Li, Nabeel B Nabulsi, Shannan Henry, Ming-Qiang Zheng, Zhengxin Cai, Hong Gao, Michael Kapinos, David Labaree, Jim Ropchan, David Matuskey, Yiyun Huang, and Richard E. Carson
*PET Center, Yale School of Medicine, CT, USA*

## Synaptic Vesicle glycoprotein 2A (SV2A)

- **Enables the quantification of synaptic density**
- **Current SV2A tracer in human use: $^{11}$C-UCB-J**
- **$^{18}$F-SynVesT-1: Similar kinetic properties to $^{11}$C-UCB-J**
- **High uptake, fast kinetics, and excellent test-retest reproducibility.**

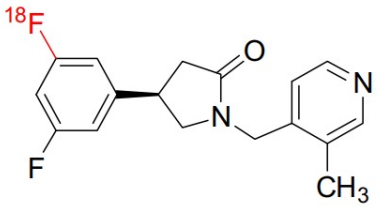


**$^{18}$F-SynVesT-1**

## Aim

**To evaluate the noninvasive model Simplified Reference Tissue Model 2 (SRTM2) to estimate $^{18}$F-SynVesT-1 binding**

Presentation #2432, SS41

Tue, June 14 3:36-3:48 114/115

## Acquisition

- 8 healthy male subjects (6 subjects: test-retest)
- 120 min dynamic PET scans on HRRT using $^{18}$F-SynVesT-1

## Models and parameters

- 4 kinetic models
  1. One-tissue compartment model (1TC, gold standard)
  2. SRTM
  3. SRTMC (reference $k_2$ parameter coupled fit)
  4. SRTM2 (reference $k_2$ = population average 1TC $k_2$)
- 2 outcome measures:
  $BP_{ND}$ (ref: Centrum semiovale) & $DVR$ (ref: cerebellum)
- Test-retest variability
- Time stability

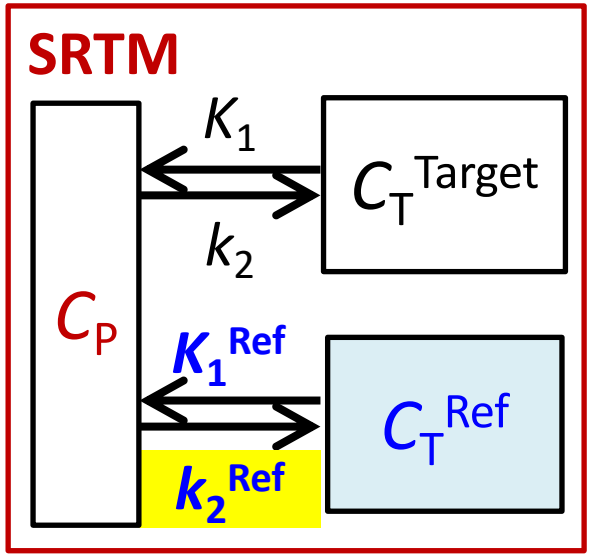


## SRTM2

$k_2^{Ref}$ = mean 1TC $k_2$ (population value)

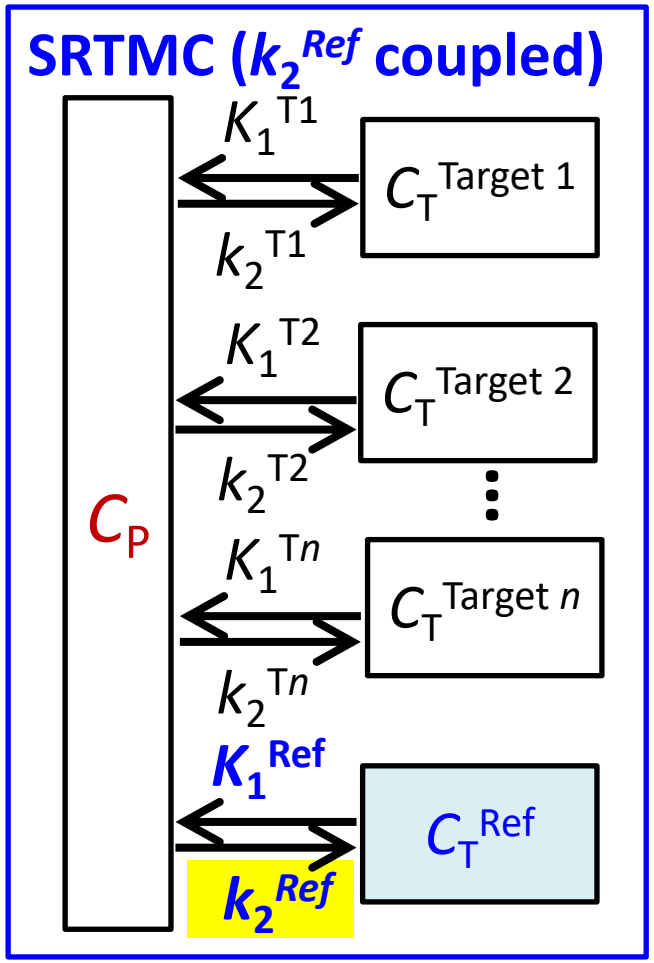

Presentation #2432, SS41

Tue, June 14 3:36-3:48 114/115

***BP*$_{ND}$**

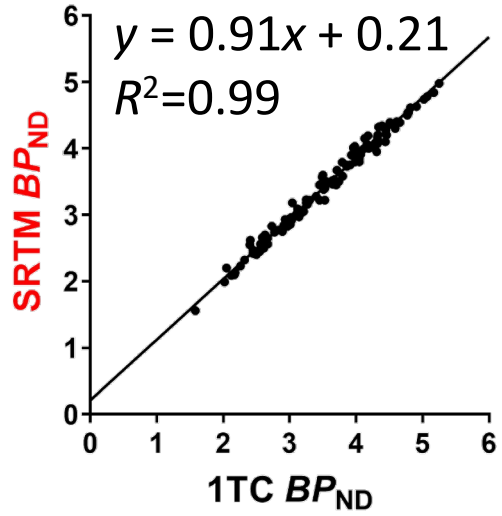


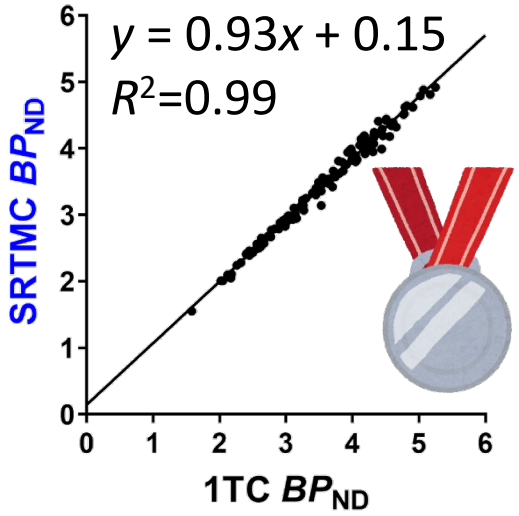


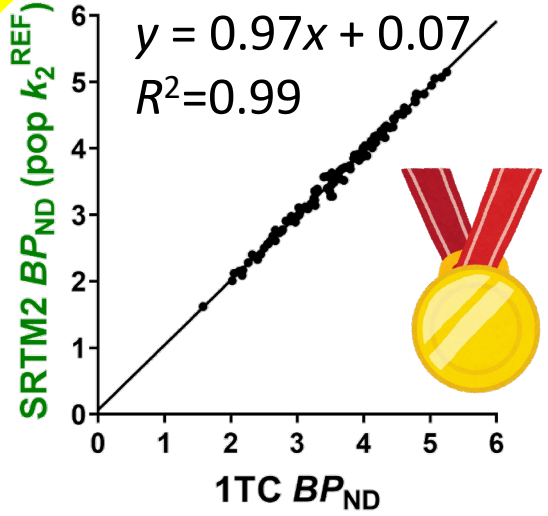


***DVR***

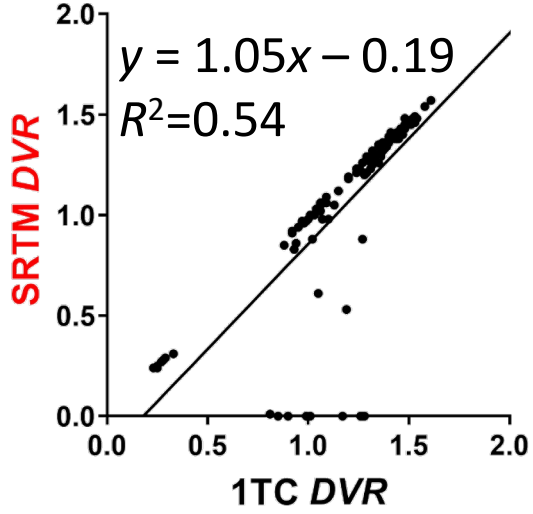


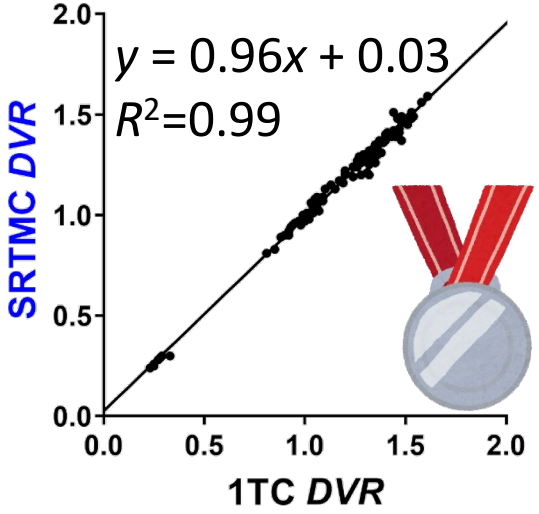


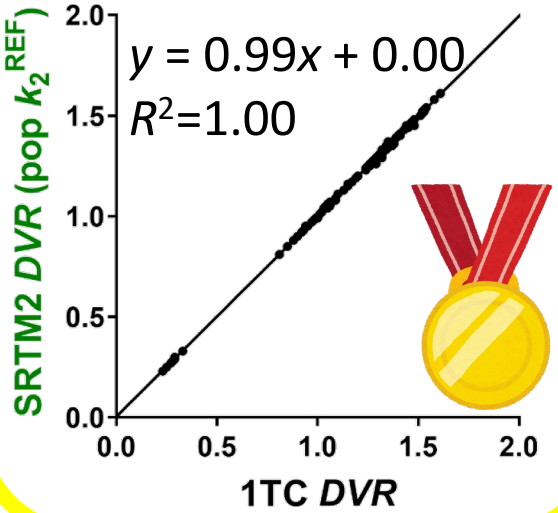


**Conclusion: The SRTM2 with population $k_2^{REF}$ value provided the best estimation of *BP*$_{ND}$ (ref: centrum semiovale) and *DVR* (ref: cerebellum) of $^{18}$F-SynVesT-1.**

Presentation #2430, SS41
Tue, June 14 3:12-3:24 114/115

# Simplified quantification for $^{18}$F-FE-PE2I: Can we do better than *SUVR*?

Praveen Honhar, David Matuskey, Richard Carson, Ansel Hillmer

Yale PET Center

Distribution Volume Ratio (*DVR*) is often approximated using the Standard Uptake Value Ratio (*SUVR*). *SUVR*, typically calculated from a late time window of PET data, can be biased with respect to *DVR*, due to non-equilibrium effects such as tracer clearance.

*Aim of the study*: **To validate a method which can correct for the bias in estimation of *DVR* by *SUVR* for $^{18}$F-FE-PE2I.**

Presentation #2430, SS41

Tue, June 14 3:12-3:24 114/115

# Methods

Our correction formula takes the following form:

$$SUVR_C = \frac{SUVR\, k_{2,\mathrm{ref}}}{k_{2,\mathrm{ref}} - \beta_{\mathrm{ref}} + \frac{SUVR\, \beta_T}{R_1}}$$

Here,

- $k_{2,\mathrm{ref}}$ : population-based $k'_2$ parameter from SRTM model
- $SUVR$ : calculated from 40-60 min post-injection (p.i.)
- $\beta_{\mathrm{ref}}$ : clearance rate of the tracer from the reference region 40-60 min p.i.
- $\beta_T$ : clearance of the tracer from the target region; difficult to estimate
- $R_1$ : relative delivery parameter, typically $R_1 \sim 1$
- $SUVR_C$ : corrected $SUVR$

# Validation

- Correction approach tested on $^{18}$F-FE-PE2I, a tracer for dopamine transporter (DAT).
- 32 human subjects [12 HCs, 20 Parkinson's disease]- dynamic brain PET scan on HRRT following a bolus of $^{18}$F- FE-PE2I.
- Ground truth *DVR* calculated from SRTM fit to 1 h PET data (*ref*=Cerebellum).
- *SUVR* - based on time window 40-60 min post-injection.
- $SUVR_C$ evaluated at regional and voxel level, results compared to *DVR*.

Presentation #2430, SS41

Tue, June 14 3:12-3:24 114/115

# Results and Conclusions

Healthy Controls (N=12)

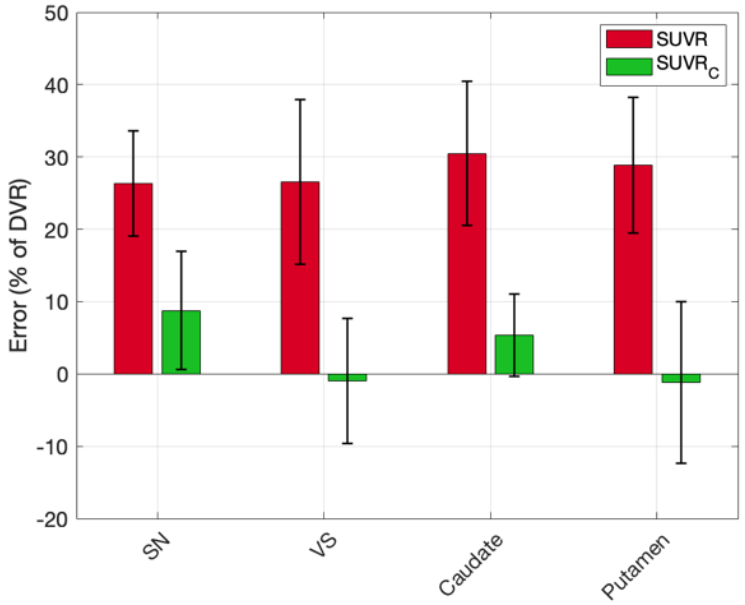


Parkinson's Disease Subjects (N=20)

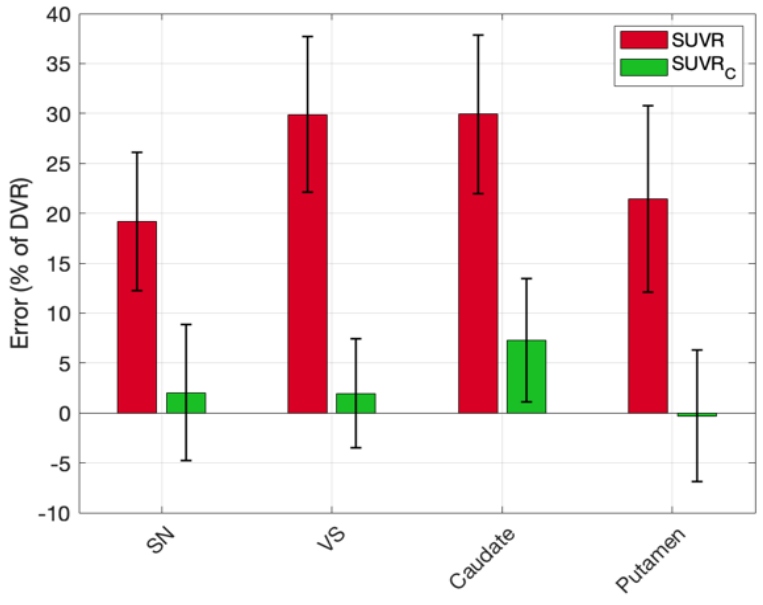


Fig 1: Correction formula ($SUVR_C$, green bars) **significantly reduces the bias and variance** in regional *DVR* estimation compared to (*SUVR*, red bars). $P < 0.0001$ for all brain regions. SN = Substantia Nigra, VS = Ventral Striatum.

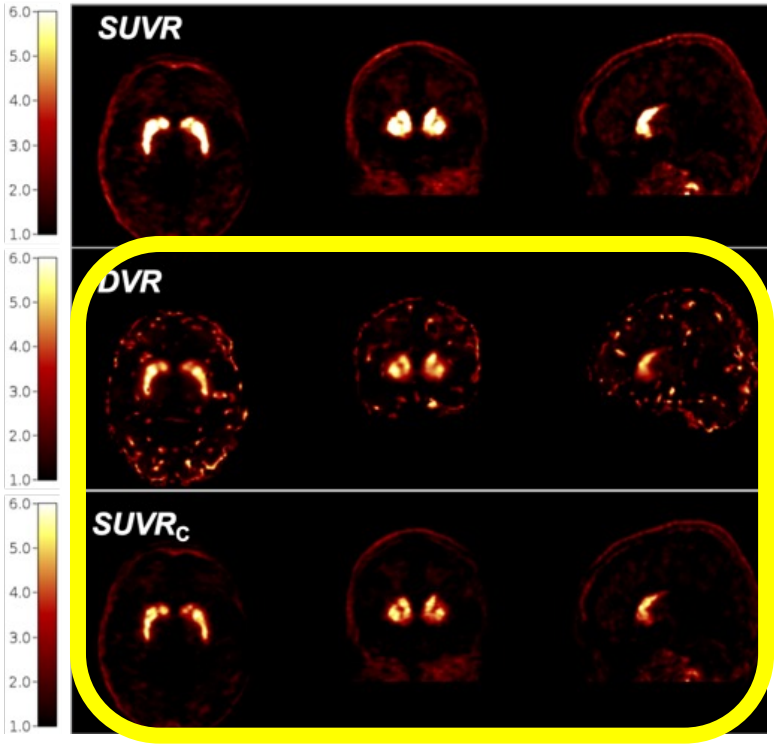


Fig 2: Performance of correction formula applied at the voxel level. *SUVR* overestimates *DVR*, $SUVR_C$ is visually similar to *DVR*. Identical color bar for all three images.

**Conclusion:** The correction approach described here **significantly reduces the bias and variability in *DVR* estimation by *SUVR*, for $^{18}$F-FE-PE2I.**


June 11-14
2022
SNMMI ANNUAL MEETING
Vancouver, British Columbia, Canada

# Cardiac

Presentation #2434, SS41

Tue, June 14 4:00-4:12 114/115

# Right Ventricular Segmentation and Quantification Using Spherical Model in Myocardial Perfusion SPECT Imaging: A Phantom and Patients Study

Negar Shahamiri[1], Mehran Yazdi[2], Mohammad Entezarmahdi[3,4], Mahdi Haghighatafshar[5], Isaac Shiri[6]

[1]Department of Computer Science and Engineering and IT, Shiraz University, [2]School of Electrical and Computer Engineering, Shiraz University, [3]Nuclear Engineering Department, Shiraz University Division of Nuclear Medicine, [4]Namazi Hospital, Shiraz University of Medical Science, [5]Nuclear Medicine and Molecular Imaging Research Center, [6]Division of Nuclear Medicine and Molecular Imaging, Geneva University Hospital

Aim of the study: Propose a **spherical model** for segmenting and quantifying the right ventricle in myocardial perfusion SPECT.

Presentation #2434, SS41
Tue, June 14 4:00-4:12 114/115

# Methods

- We found that the **spherical model outperforms ellipsoidal model** in segmenting the right ventricle specially in the HLA view, in non-gated SPECT MPI.

- The spherical model's suitability will be shown in the presentation.

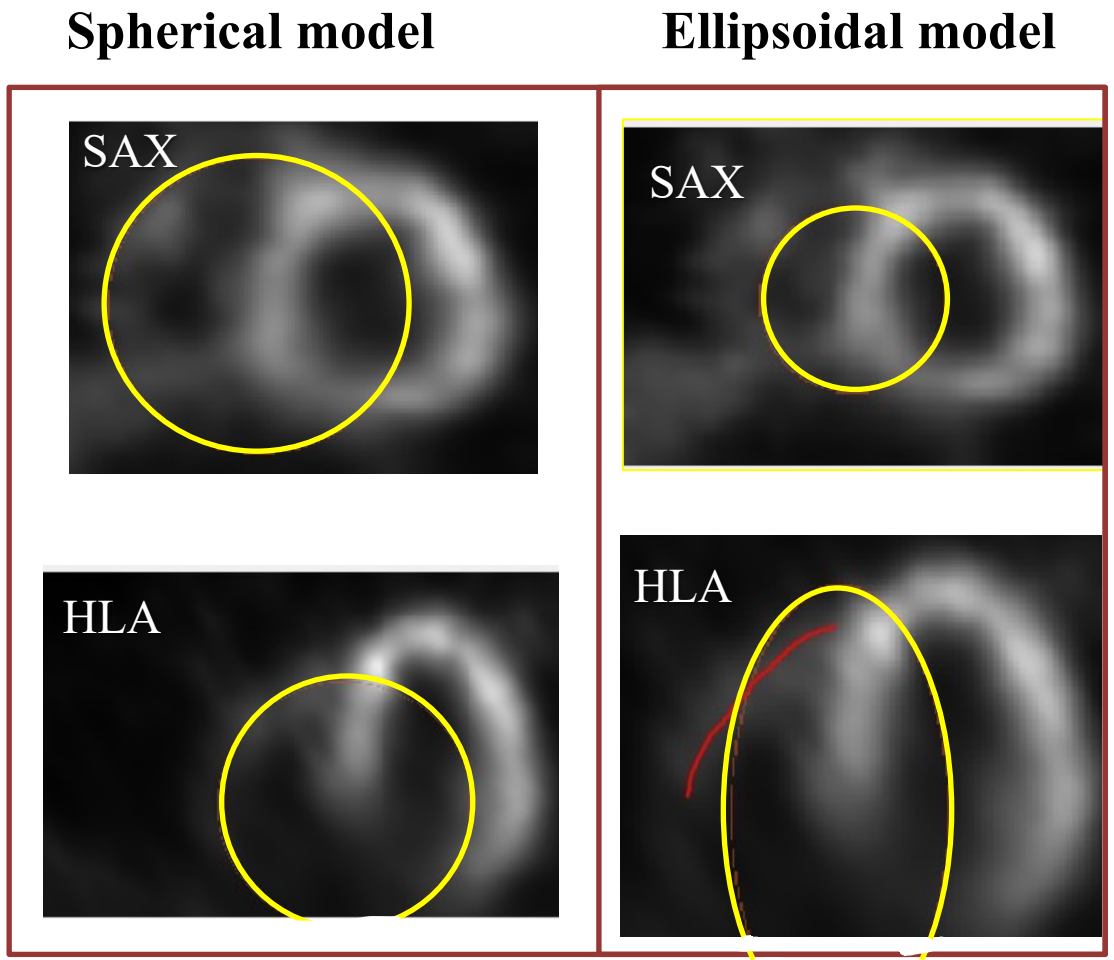

Presentation #2434, SS41

Tue, June 14 4:00-4:12 114/115

# Results and Conclusions

| Mean Absolute Error in RV cavity volume (Phantom Study) | |
|---|---|
| **QPS** (Cedars Sinai Package) | **Proposed** (Spherical Model) |
| 107% | **5%** |

| Accuracy of proposed method (Patient Study, n=70 with 37 with RCA stenosis) |
|---|
| Prediction of Right Coronary Artery Stenosis with MPI |
| **71.5%** |

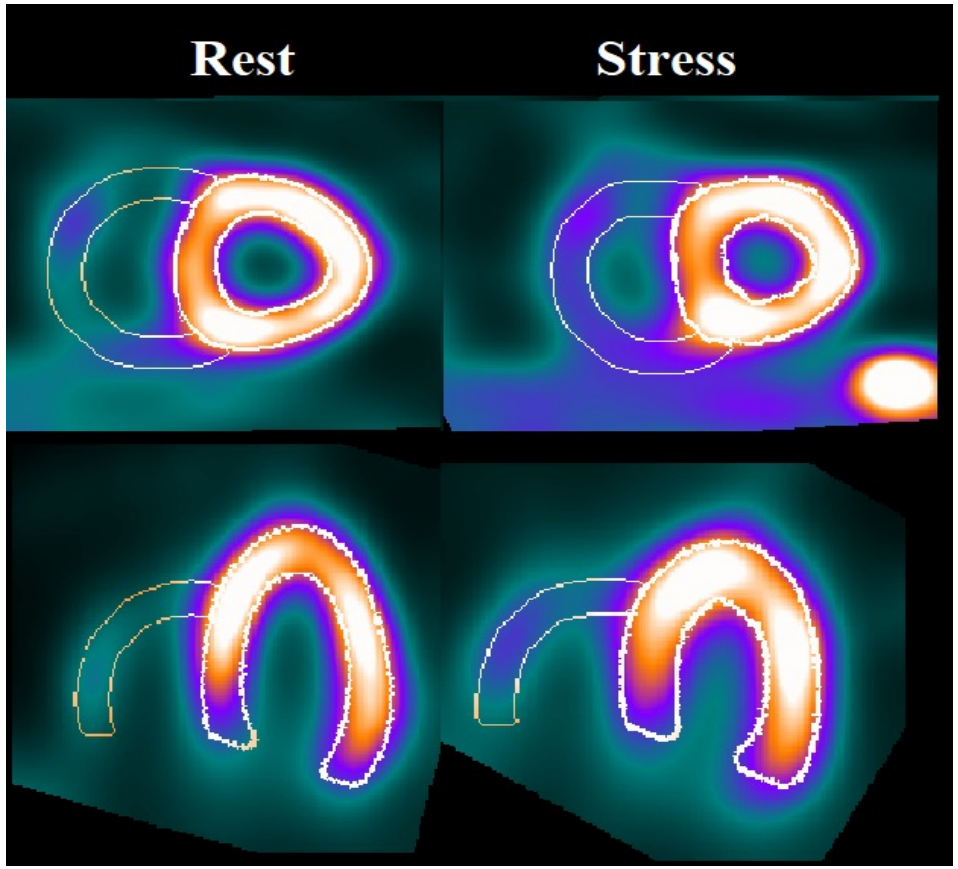


**A spherical model outperforms a commercial software for RV segmentation**

# Long-axial FOV and Total body PET

Presentation #3192, PIDS Poster

Sat, June 11 6:00-8:00 PM Hall A

# Shortened whole body dynamic PET $^{18}$F-FDG Patlak imaging using a population input function and the Biograph Vision Quadra PET/CT

Joyce van Sluis[1], Paul H. van Snick[1], Adrienne H. Brouwers[1], Walter Noordzij[1], Rudi A.J.O. Dierckx[1], Ronald J.H. Borra[1], Adriaan A. Lammertsma[1], Andor W.J.M. Glaudemans[1], Maqsood Yaqub[2], Charalampos Tsoumpas[1], and Ronald Boellaard[1,2]

[1] *University Medical Center Groningen, University of Groningen, Groningen, The Netherlands*

[2] *Amsterdam University Medical Centers, location VUMC, Amsterdam, The Netherlands*

Aim of the study: to apply Patlak analysis of whole body 18F-FDG images using the Vision Quadra, including the use of a population-averaged input function to allow for shortened scan durations for more clinically pragmatic implementation

Presentation #3192, PIDS Poster

Sat, June 11 6:00-8:00 PM Hall A

# Methods

- 12 patients received a 3 MBq/kg weight-based injection of $^{18}$F-FDG
- 65 min dynamic PET acquisitions were performed, and studies were reconstructed using **E**uropean **A**ssociation of Nuclear Medicine **R**esearch **L**td. (**EARL**) standards 2 reconstruction settings
- VOIs were placed in the ascending aorta (AA) to obtain IDIF
- Subsequently, PIF was scaled to AA IDIF values at 30-60, 40-60, and 50-60 min p.i.

Parametric $^{18}$F-FDG *Ki* images were generated:

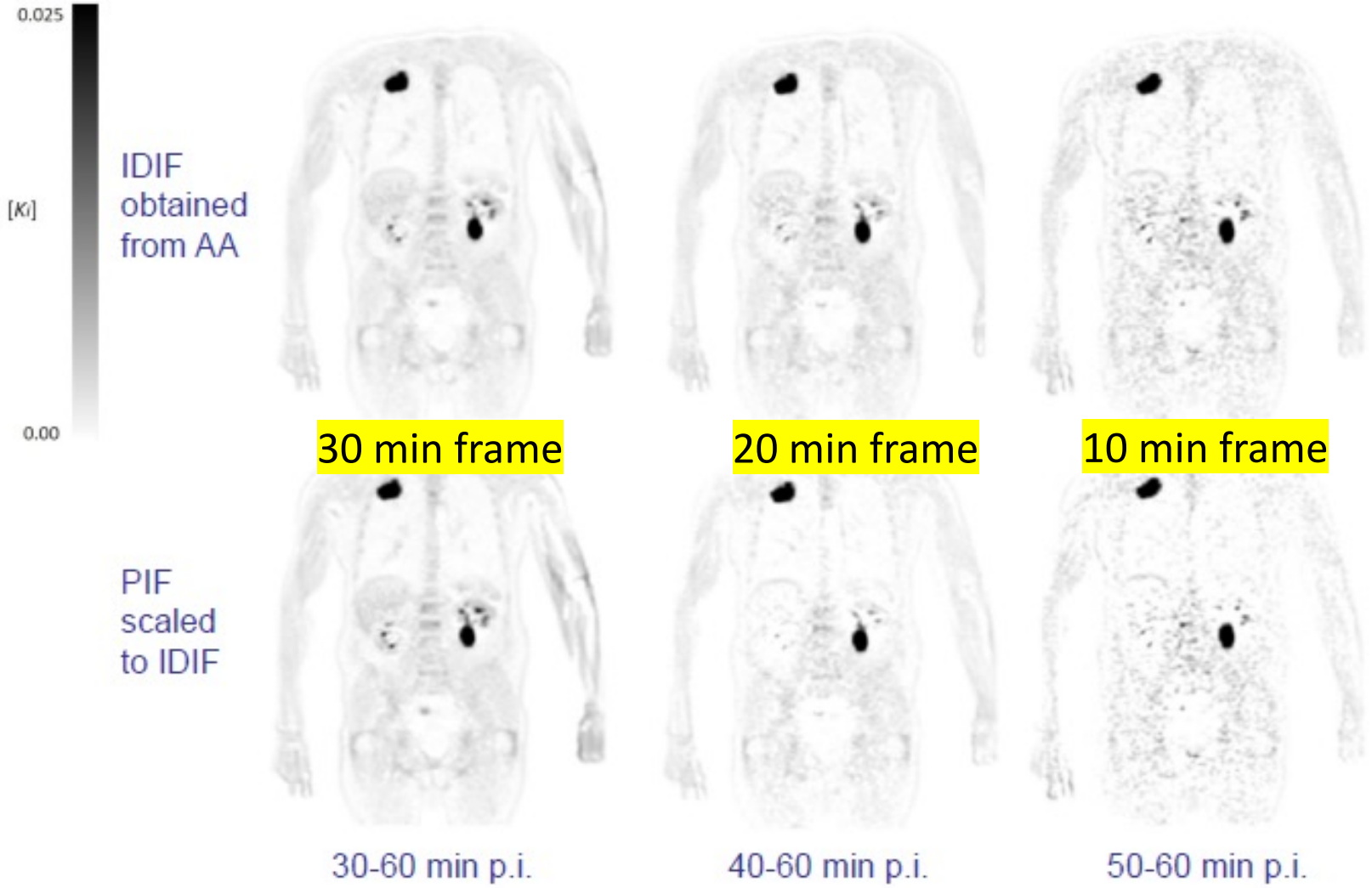

Presentation #3192, PIDS Poster

Sat, June 11 6:00-8:00 PM Hall A

# Results and Conclusions

- Good agreement between the AA IDIF and PIF scaled to 30-60 min p.i. and 40-60min p.i. was obtained with <8% deviation in *Ki*
- Bland-Altman plots showed excellent agreement in *Ki* obtained using the PIF scaled to the IDIF at 30-60 min p.i. and at 40-60 min p.i.

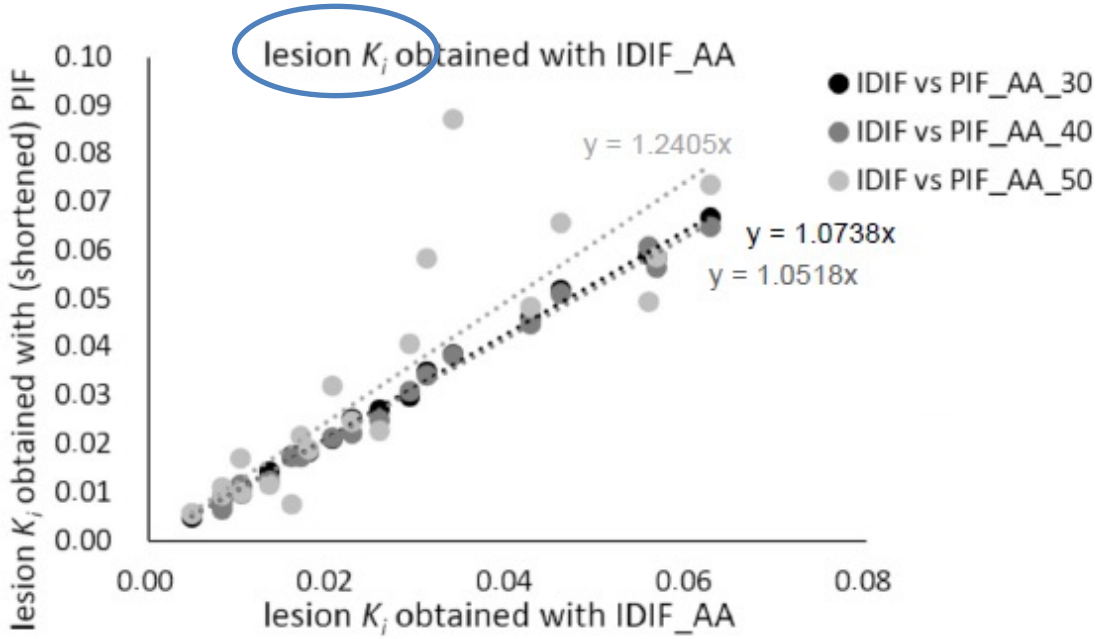


**Whole body dynamic Patlak imaging is feasible using shortened scan time interval at 40-60 min p.i.**

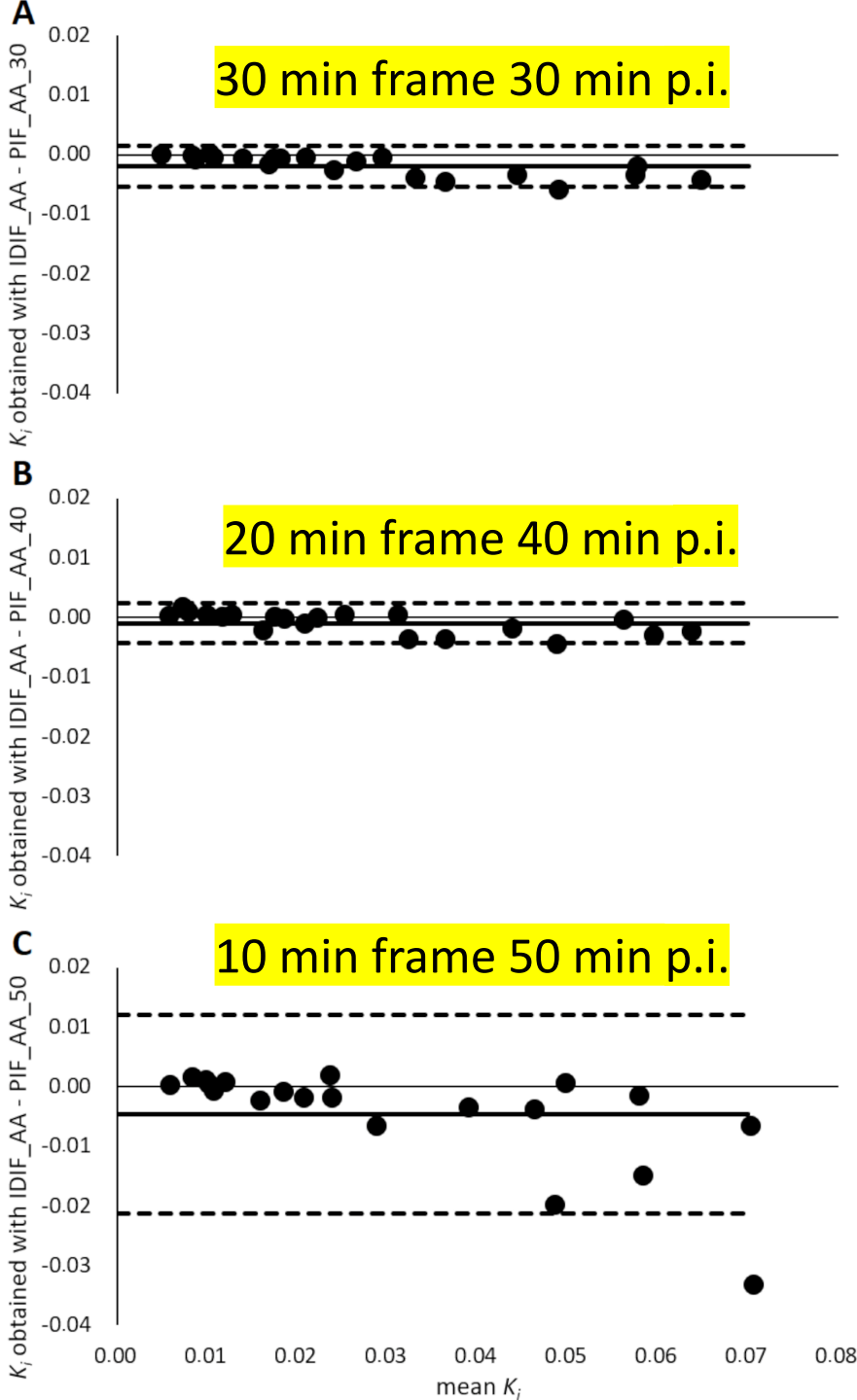

Presentation #3183, PIDS Poster

Sat, June 11 6:00-8:00 PM Hall A

# Evaluation of population-based input functions for kinetic modelling of 18F-FDG datasets from a long axial FOV PET scanner

Hasan Sari[1,2], Lars Eriksson[3,4], Clemens Mingels[2], Michael E. Casey[3], Paul Cumming[2], Ian Alberts[2], Kuangyu Shi[2], Maurizio Conti[3], Axel Rominger[2]

1. Advanced Clinical Imaging Technology, Siemens Healthcare AG, Lausanne, Switzerland
2. Department of Nuclear Medicine, Inselspital, Bern University Hospital, University of Bern, Switzerland
3. Siemens Medical Solutions USA, Inc., Knoxville, USA

Aim of the study: To exploit the high sensitivity of a LAFOV PET system to explore the applicability of PBIF with abbreviated acquisition procotols for $^{18}$F-FDG total-body parametric imaging.

Presentation #3183, PIDS Poster

Sat, June 11 6:00-8:00 PM Hall A

# Methods

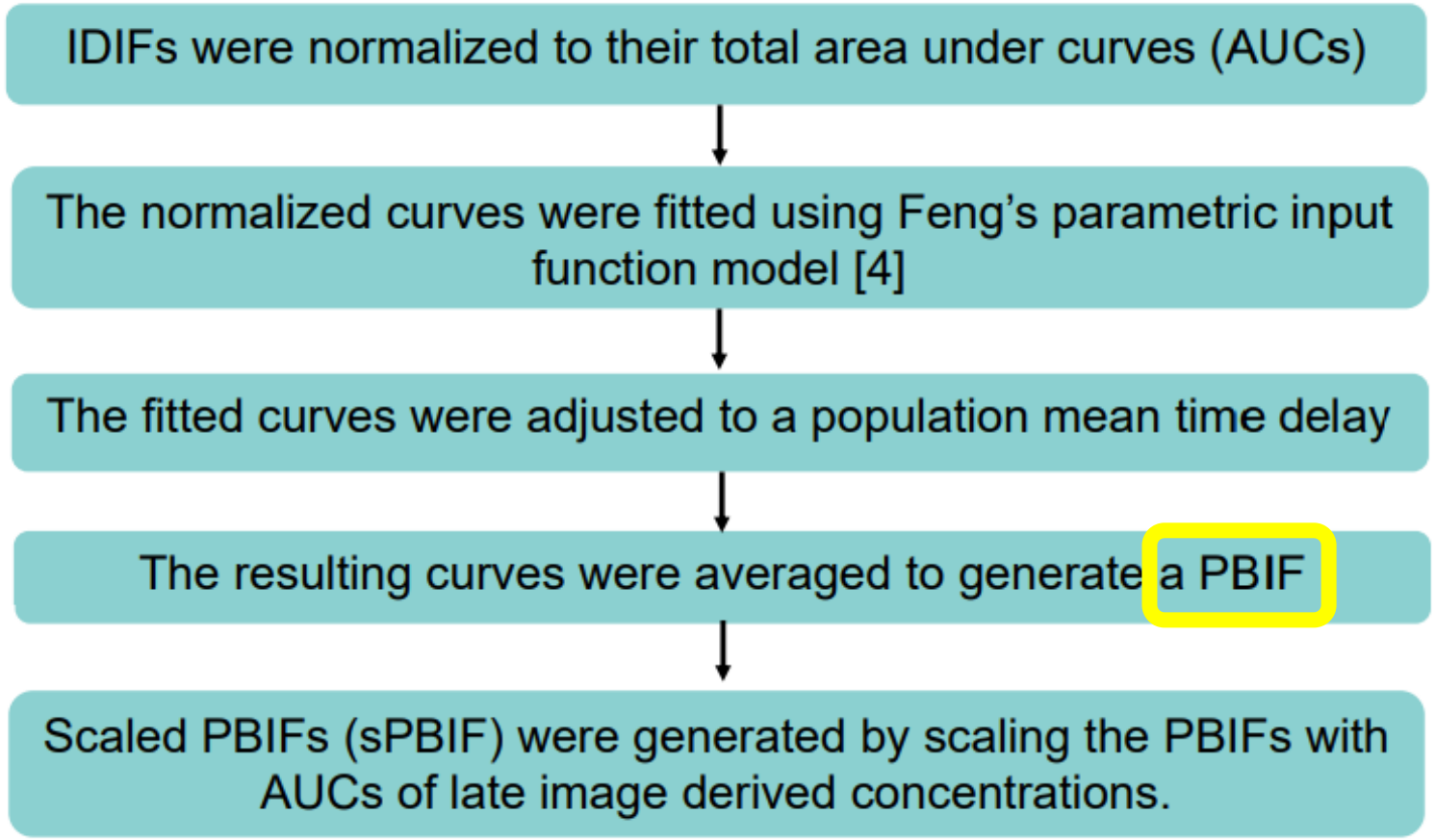


- The performance of sPBIFs and abbreviated protocols were evaluated against IDIF by comparing Patlak $K_i$ estimates in tumour lesions and cerebral grey matter.

Presentation #3183, PIDS Poster

Sat, June 11 6:00-8:00 PM Hall A

# Results and Conclusions

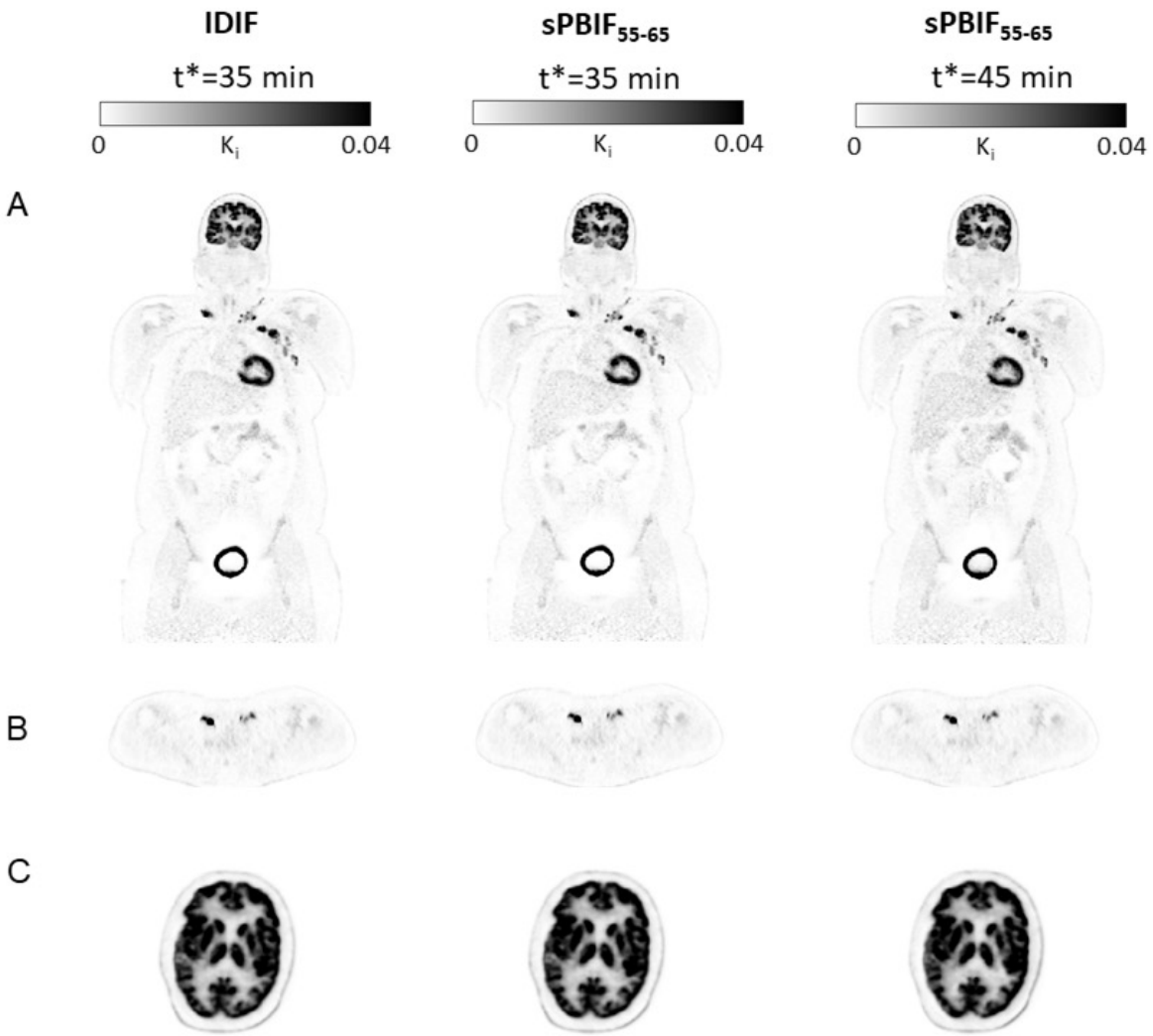


*Quite consistent with the previous presentation*

This study demonstrate that with a sPBIF, 20 minutes of PET data (45-65 min p.i.) might be adequate for accurate kinetic modelling of tumour lesions, versus only 15 minutes (50-65 min p.i.) for brain grey matter.

Presentation #3193, PIDS Poster

Sat, June 11 6:00-8:00 PM Hall A

中国科学院深圳先进技术研究院
SHENZHEN INSTITUTES OF ADVANCED TECHNOLOGY
CHINESE ACADEMY OF SCIENCES

# Comparison between a dual-time-window protocol and other simplified protocols for dynamic total-body $^{18}$F-FDG PET imaging

**Zhenguo Wang[1], Yaping Wu[2], Yongfeng Yang[1], Meiyun Wang[2], Tao Sun[1]**

1. Paul C. Lauterbur Research Center for Biomedical Imaging, Shenzhen Institute of Advanced Technology, Chinese Academy of Sciences, Shenzhen, People's Republic of China
2. Henan Provincial People's Hospital and the People's Hospital of Zhengzhou, University of Zhengzhou, People's Republic of China

**Aim of the study:**

- Propose a dual-time-window (DTW) protocol for a dynamic total-body $^{18}$F-FDG PET scan to reduce the scan time while obtaining multiple kinetic parameters.
- Compare the proposed DTW protocol with other existing simplified protocols.

Presentation #3193, PIDS Poster

Sat, June 11 6:00-8:00 PM Hall A

中国科学院深圳先进技术研究院
SHENZHEN INSTITUTES OF ADVANCED TECHNOLOGY
CHINESE ACADEMY OF SCIENCES

## Proposed DTW protocol

- **Image acquisition (uExplorer):** an early acquisition performed after injection for 10 minutes and a late acquisition after a break with a fixed end time of 60 minutes.
- **Estimation of the missing TACs:** nonlinear data completion (3rd degree rational function)
- **Input function:** a combination of IDIF (image derived input function) and PBIF (population-based input function)
- **2TCM fitting:** apply Lawson-Hanson non-negative least squares algorithm to accelerate the voxelized modelling

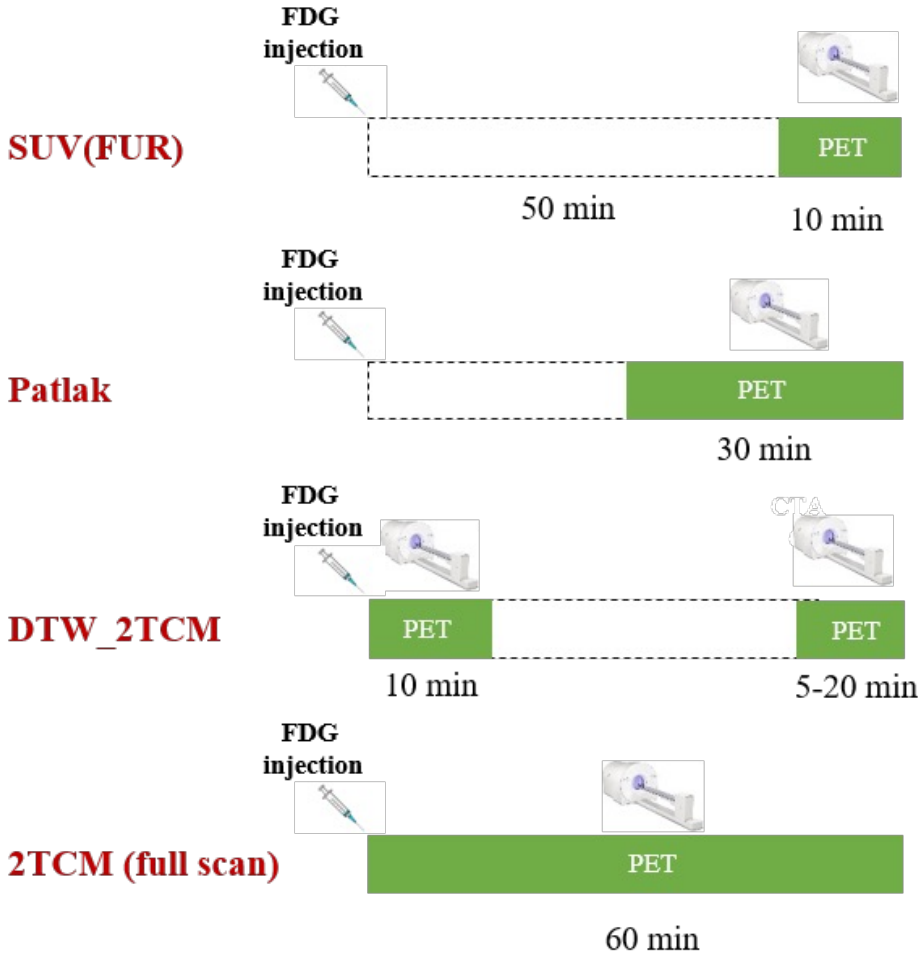


## Assessment:

- Both **ROI-based quantification** and **parametric images**
- Compare with **Patlak**, **SUV, Fractional Uptake Ratio (FUR)**
- Parameters from full scan as the reference

Presentation #3193, PIDS Poster

Sat, June 11 6:00-8:00 PM Hall A

中国科学院深圳先进技术研究院
SHENZHEN INSTITUTES OF ADVANCED TECHNOLOGY
CHINESE ACADEMY OF SCIENCES

| | Cerebral cortex | Muscle | Tumor |
|---|---|---|---|
| **DTW $K_i$** | **$R^2$=0.971** | **$R^2$=0.990** | **$R^2$=0.990** |
| **(10+5 min)** | **p<0.001** | **p<0.001** | **p<0.001** |
| **Patlak $K_i$** | $R^2$=0.961 | $R^2$=0.863 | $R^2$=0.990 |
| **(30–60 min)** | p<0.001 | p<0.001 | p<0.001 |
| **FUR** | $R^2$=0.967 | $R^2$=0.937 | $R^2$=0.972 |
| **(50–60 min)** | p<0.001 | p<0.001 | p<0.001 |
| **SUV** | $R^2$=0.447 | $R^2$=0.729 | $R^2$=0.390 |
| **(50–60 min)** | p=0.002 | p<0.001 | p=0.054 |

**Table.** Correlation analysis for $K_i$ and its surrogate by different quantification methods

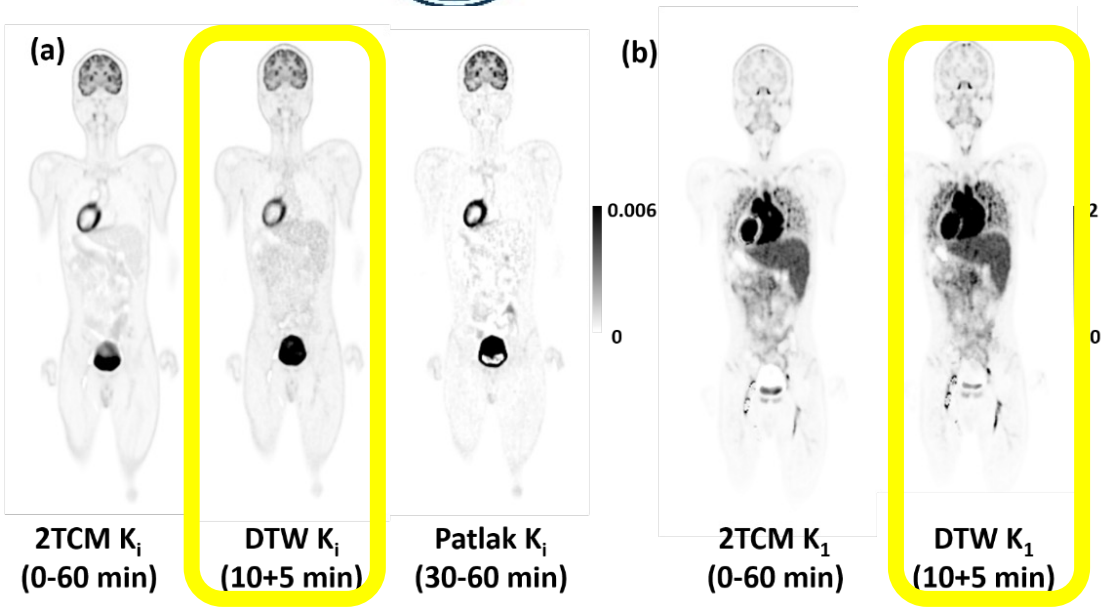


**Figure**. Whole-body parametric images: (a) $K_i$ images generated from the 60-min full scan, the DTW protocol (10+5 min), and Patlak analysis; (b) $K_1$ images generated from the 60-min scan and the DTW protocol (10+5 min).

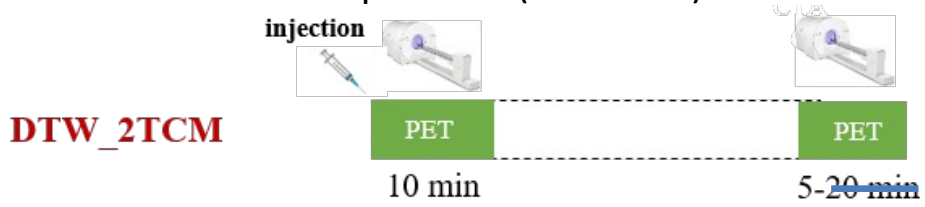


**Conclusion**：With a total scan time of 15 minutes, DTW protocol can obtain accurate $K_i$ and $K_1$ quantification and acceptable visual performance in parametric images; different simplified protocol may be suitable for specific application.

Presentation #3185, PIDS Poster

Sat, June 11 6:00-8:00 PM Hall A

# Feasibility of Standard and Generalized Patlak Models for Dynamic Imaging of Multiple Organs using the uEXPLORER PET Scanner

Fengyun Gu[1,2], Qi Wu[1,2], Jianmao Wu[3], Debin Hu[1], Tianyi Xu[1], Shuangliang Cao[1], Yun Zhou[1], Hongcheng Shi[3]

1. United Imaging Healthcare, Shanghai, China;
2. Department of Statistics, University College Cork, Cork, Ireland;
3. Department of Nuclear Medicine, Zhongshan Hospital, Fudan University, Shanghai, China

Aim of the study: to investigate the feasibility of standard and generalized Patlak models for diverse tissues.

Presentation #3185, PIDS Poster

Sat, June 11 6:00-8:00 PM Hall A

# Methods

## A Standard Patlak Plot
**(irreversible tracers, $k_4$=0)**

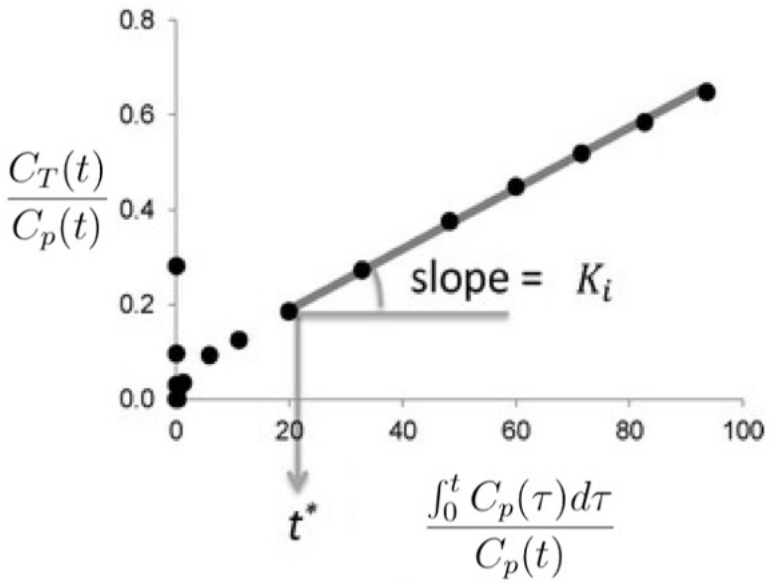


$$\frac{C_T(t)}{C_p(t)} = K_i \frac{\int_0^t C_p(\tau)d\tau}{C_p(t)} + V$$

Patlak, Clifford S, Ronald G Blasberg and Joseph D Fenstermacher. 1983. "Graphical evaluation of blood-to-brain transfer constants from multiple-time uptake data." *Journal of Cerebral Blood Flow & Metabolism* 3(1):1–7.

## B Generalized Patlak Plot
**(reversible tracers, $k_4 \neq 0$)**

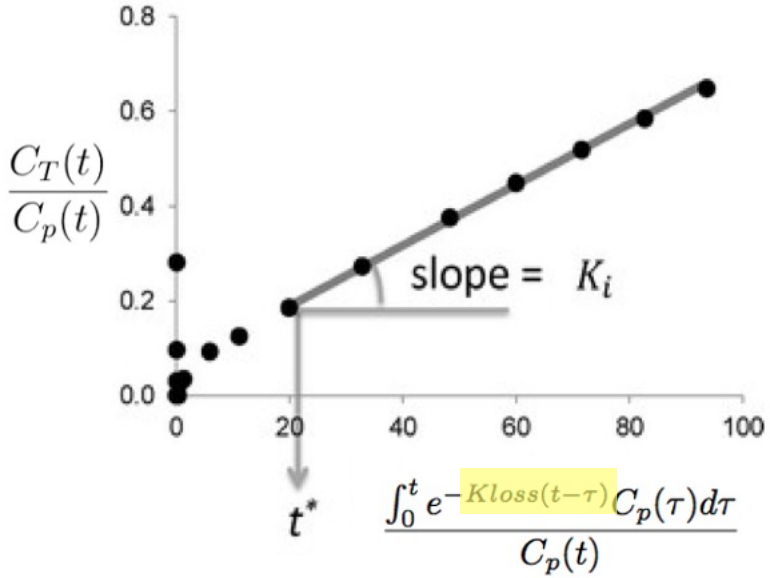


$$\frac{C_T(t)}{C_p(t)} = K_i \frac{\int_0^t e^{-Kloss(t-\tau)} C_p(\tau)d\tau}{C_p(t)} + V$$

Patlak, Clifford S and Ronald G Blasberg. 1985. "Graphical evaluation of blood-to-brain transfer constants from multiple-time uptake data. Generalizations." *Journal of Cerebral Blood Flow & Metabolism* 5(4):584–590.

Presentation #3185, PIDS Poster

Sat, June 11 6:00-8:00 PM Hall A

# Results and Conclusions

Standard Patlak

Generalized Patlak

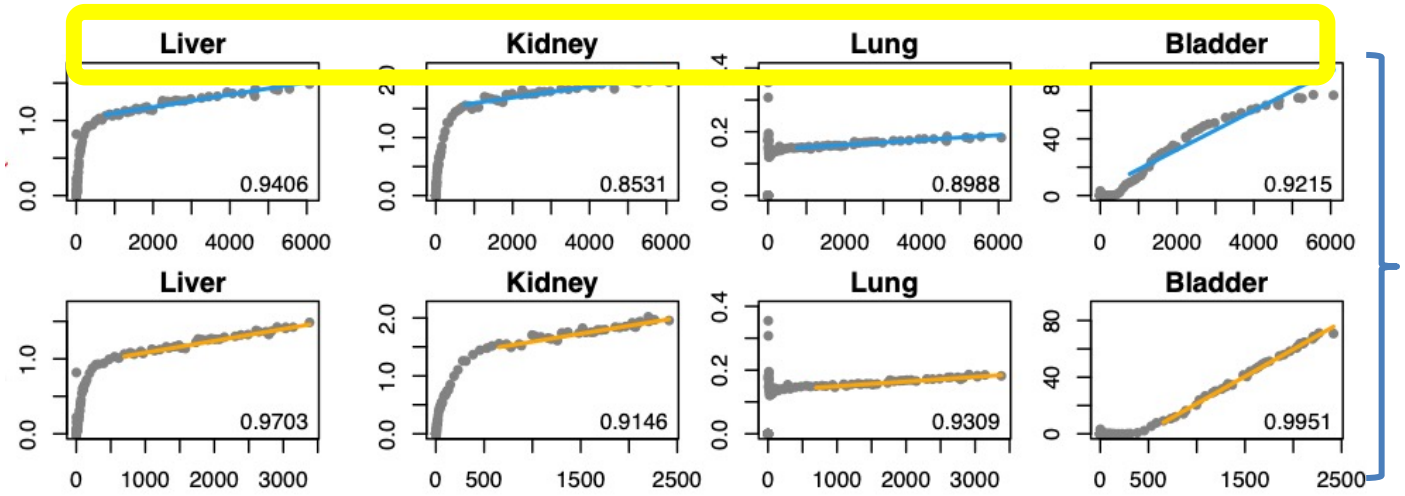


R squared is indicated in each plot.

*Potential benefit*

Standard Patlak

Generalized Patlak

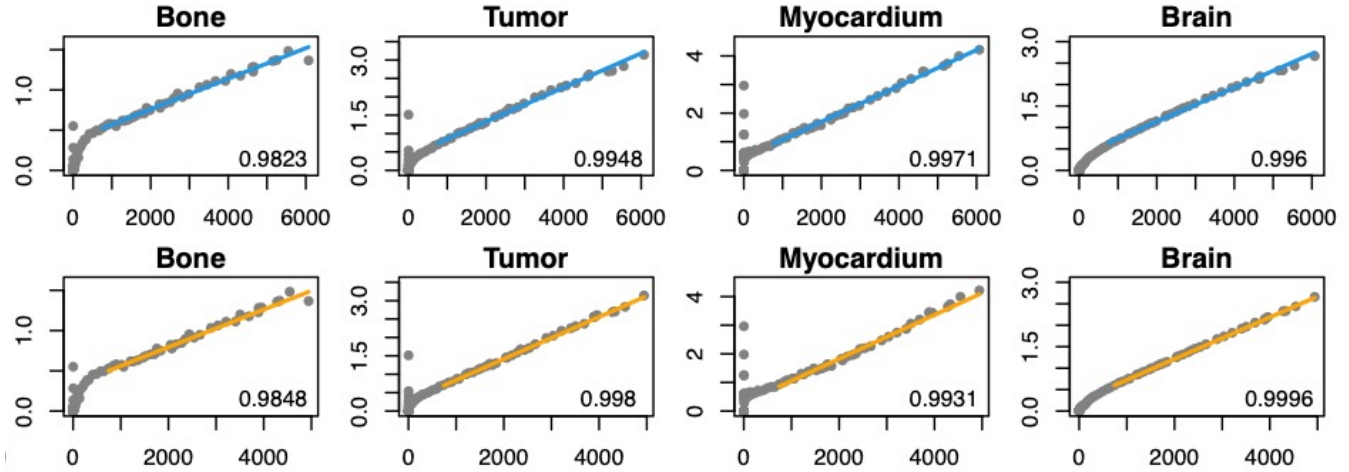


*No need to use gPatlak*

- Generalized Patlak analysis can bring some benefits for certain tissues with complex kinetic characteristics such as liver, kidney, lung, especially bladder.

Presentation #2600, IS1
Sat, June 11 2:24-2:36 205/206

UC DAVIS HEALTH

# Kernel SIME: simultaneous estimation of blood input function using a kernel method and its evaluation with total-body PET

Yansong Zhu[a], Yiran Wang[a], Quyen Tran[a], Ramsey D. Badawi[a], Simon R. Cherry[a], Jinyi Qi[a], Shiva Abbaszadeh[b], Guobao Wang[a]

[a] University of California – Davis
[b] University of California – Santa Cruz

**Aim of the study**: We developed a kernel-based simultaneous estimation (SIME) method to provide a stable and accurate blood input function for dynamic PET imaging with conventional scanners.

Presentation #2600, IS1
Sat, June 11 2:24-2:36 205/206

# Methods

**Existing noninvasive methods:**

- Image-derived input function (IDIF)
  - Suffers from partial volume effect when major blood pool is not available (e.g., in brain imaging)
- Optimization-derived input function (ODIF) using simultaneous estimation (SIME) from multiple tissue time activity curves (TACs)
  - Highly ill-posed problem and is not stable

**Proposed kernel SIME exploits IDIF as *a priori* information to stabilize ODIF.**

**Kernel SIME**

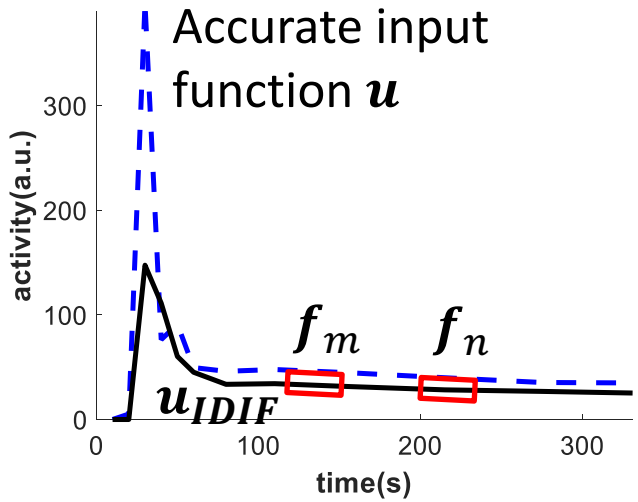


- Extract 1D feature maps (e.g. $\boldsymbol{f}_m, \boldsymbol{f}_n$) from $\boldsymbol{u}_{IDIF}$ to build a kernel matrix
- Kernel representation of blood input function:

$$u_m = \sum_n \alpha_n \kappa_{IDIF}(\boldsymbol{f}_m, \boldsymbol{f}_n)$$

- Estimate the kernel coefficients $\boldsymbol{\alpha}$ jointly with kinetic parameters

Presentation #2600, IS1

Sat, June 11 2:24-2:36 205/206

# Results and Conclusions

- Evaluation on dataset from uEXPLORER total body PET/CT system, which allows extracting a reference input function from the heart for comparison.

**Estimated input functions**

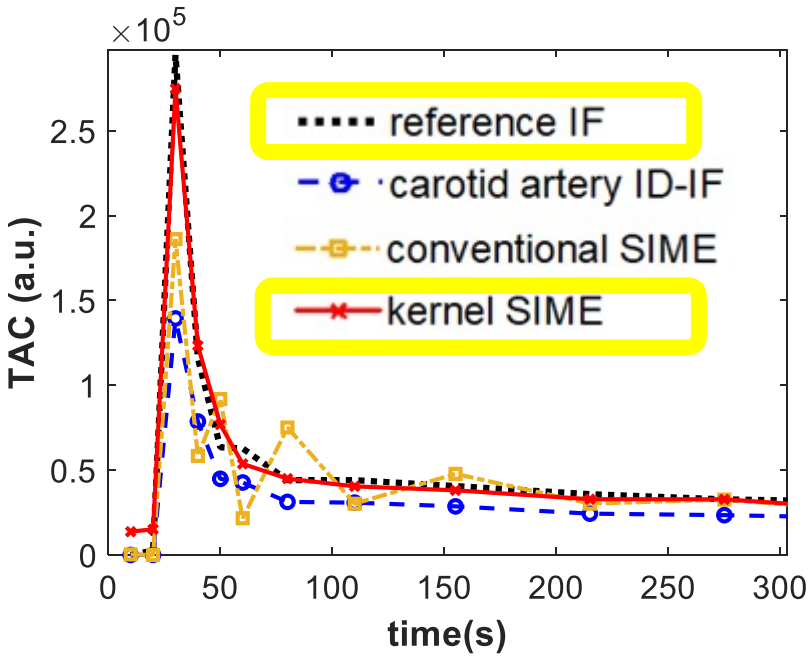


**Impact on kinetic parameters**

Mean absolute error (MAE)

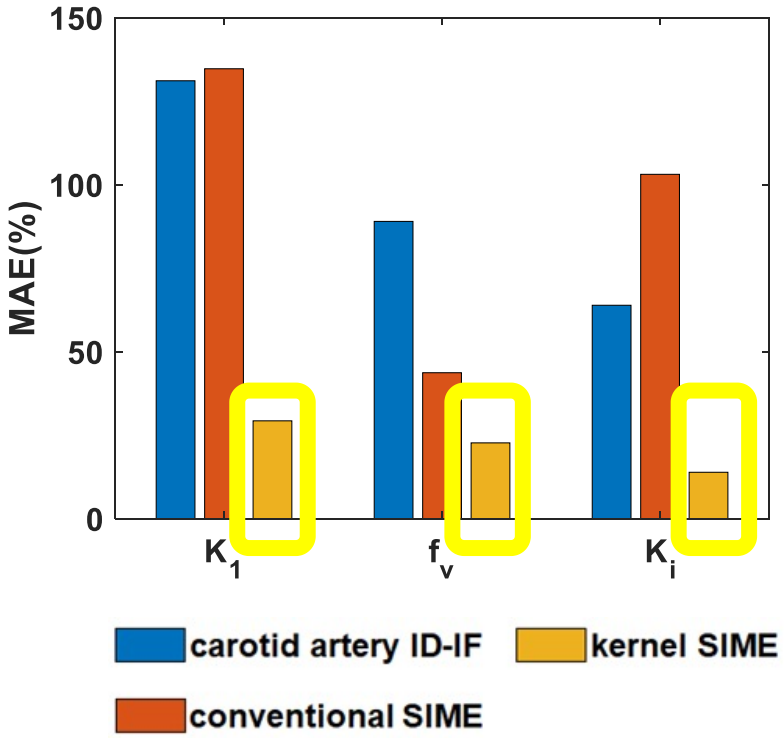


**Impact on $K_i$ images**

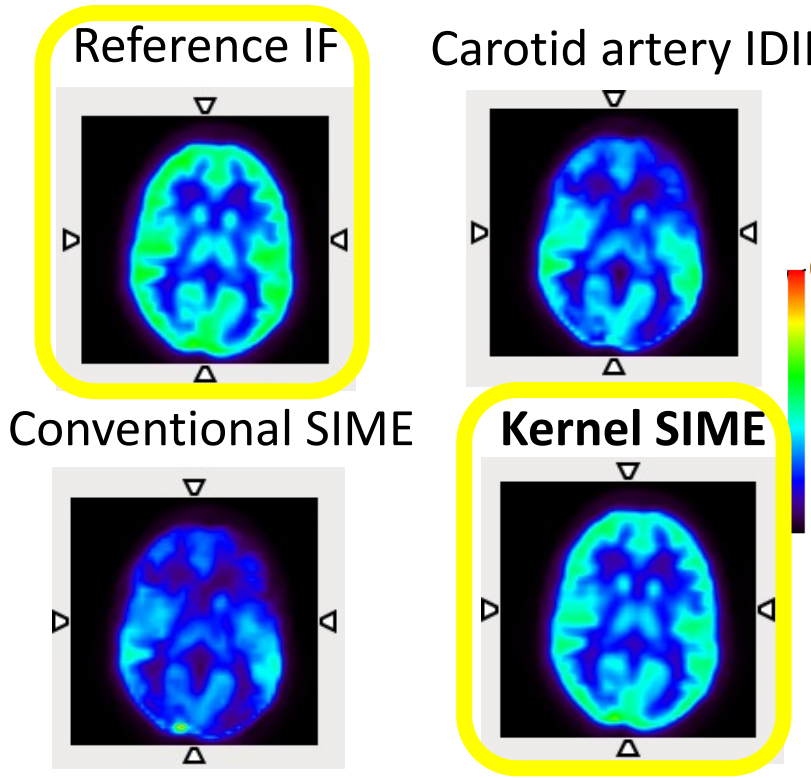


⚠ *A late blood sample is still needed*

**Conclusion: The proposed kernel SIME enables more accurate estimation of input function and kinetic parameters for brain PET imaging as compared to conventional SIME and carotid-artery IDIF**

Presentation #2518, PIDS YIA Symposium

Sat, June 11 4:03-4:15 109

Highest score in DAM

# High-Temporal Resolution Kinetic Modeling on Total-Body PET Differentiates the Hepatic Interstitial Space in Nonalcoholic Fatty Liver Disease and Healthy Subjects

Quyen Tran, Karen E. Matsukuma, Benjamin A. Spencer, Yiran Wang, Elizabeth Li, Michael T Corwin, Simon R. Cherry, Ramsey D. Badawi, Souvik Sarkar, and Guobao Wang

**University of California - Davis**

**Aim**: To demonstrate the use of high-temporal resolution dynamic PET imaging enabled on EXPLORER for modeling the interstitial space of liver in healthy and diseased subjects

# Methods

- Interstitial space is the fluid space surrounding tissue cells. However, standard two-tissue (2T) compartment model using low temporal resolution (10-20s/frame) usually overlooks the interstitial space.
- EXPLORER total-body PET enables high temporal resolution (e.g., 2s/frame), which allows to separate the free-state tissue space $C_f(t)$ of standard 2T model into the interstitial space $C_i(t)$ and intracellular space $C_e(t)$, thus a 3T model:

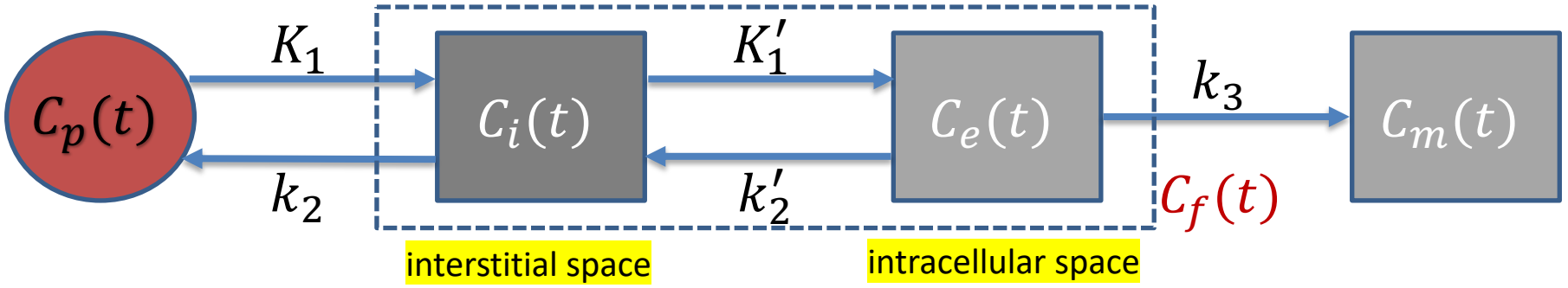


- For the liver, it is important to also model the dual-blood input function (DBIF).
- **Advantages** of the 3T model: (1) Improve quantification of the liver glucose transport rate $K_1$, and (2) enable the calculation of the liver interstitial-space distribution volume $V_x$.

# Results

Modeling of the interstitial space (i.e., the 3T model) improved the quantification of liver FDG $K_1$ for differentiating nonalcoholic steatohepatitis (NASH) from non-NASH patients

The interstitial-space distribution volume $V_x$ was also different in NASH vs. non-NASH

By 2T model

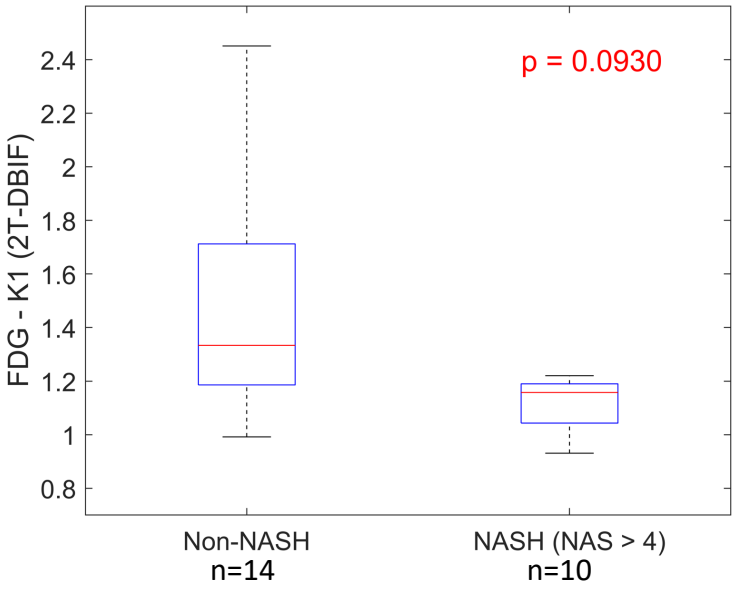


By 3T model

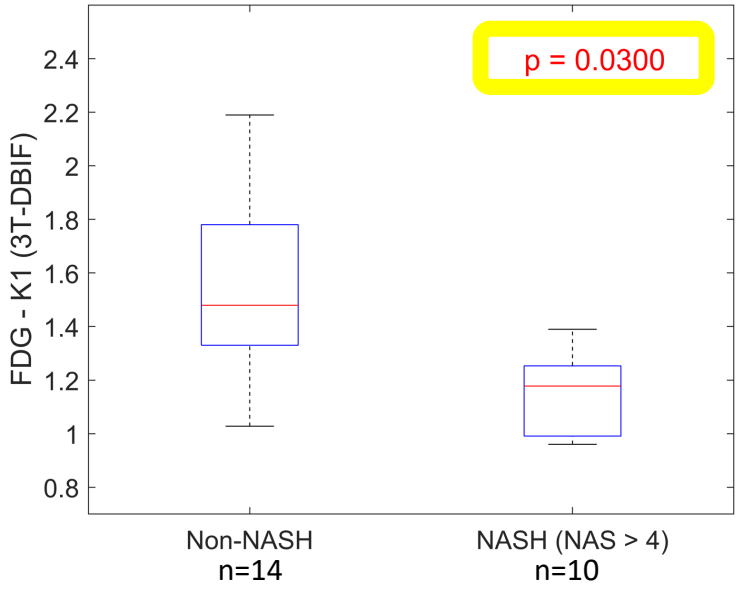


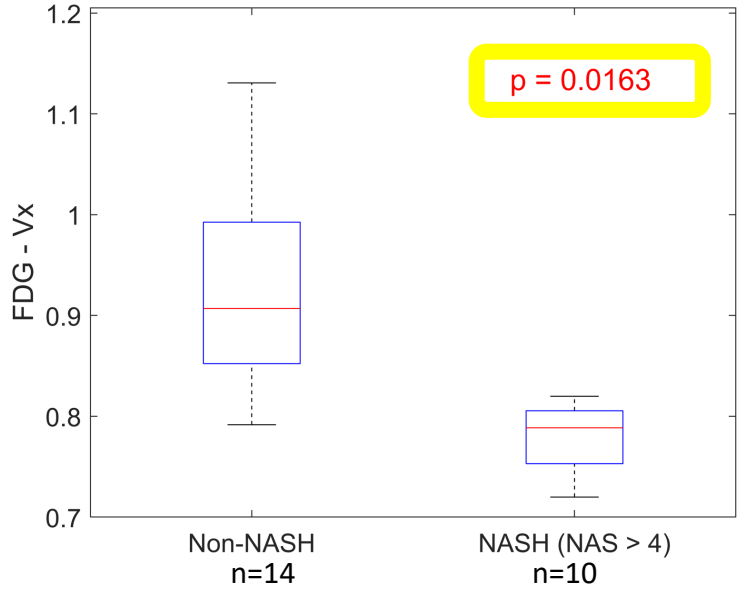


**Conclusion**: kinetic characterization of the interstitial space has the strong potential to derive multiparametric PET imaging biomarkers to assess NASH.


June 11-14
2022
SNMMI ANNUAL MEETING
Vancouver, British Columbia, Canada

# Dosimetry

Presentation #2433, SS41
Tue, June 14 3:48-4:00 114/115

# Estimation of Time-Integrated Activity Using Single Time Point Imaging, a Physiologically-Based Pharmacokinetic Model and a Nonlinear Mixed-Effects Model

*Deni Hardiansyah[1], Ade Riana[1], Ambros J. Beer[2], Gerhard Glatting[2,3]*

[1]Medical Physics and Biophysics, Physics Department, Faculty of Mathematics and Natural Sciences, Universitas Indonesia, Depok, Indonesia
[2]Department of Nuclear Medicine, Ulm University, Ulm, Germany
[3]Medical Radiation Physics, Department of Nuclear Medicine, Ulm University, Ulm, Germany

Aim of the study: To investigate the accuracy of the calculated time-integrated activity coefficients (TIACs) obtained from a single time point imaging, plus a physiologically-based pharmacokinetic (PBPK) model and a nonlinear mixed effect (NLME) approach in peptide-receptor radionuclide therapy (PRRT).

Presentation #2433, SS41

Tue, June 14 3:48-4:00 114/115

# Methods

## PBPK Model

Global Structure of the **whole-body** PBPK Model

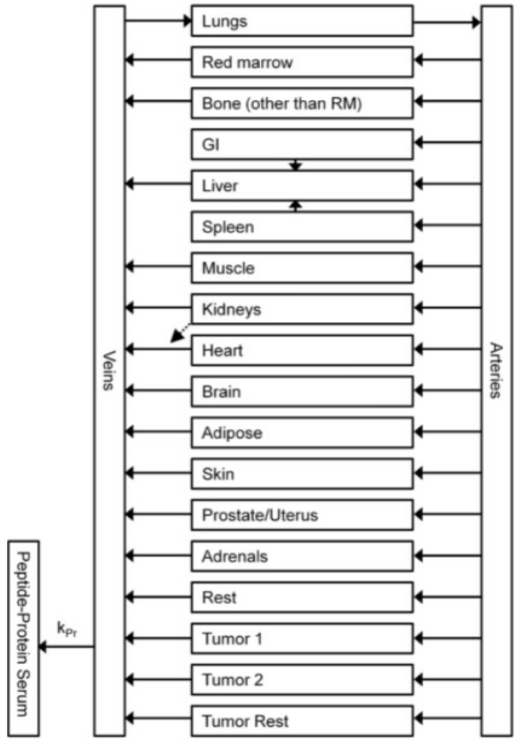


Organ structure of the PBPK model

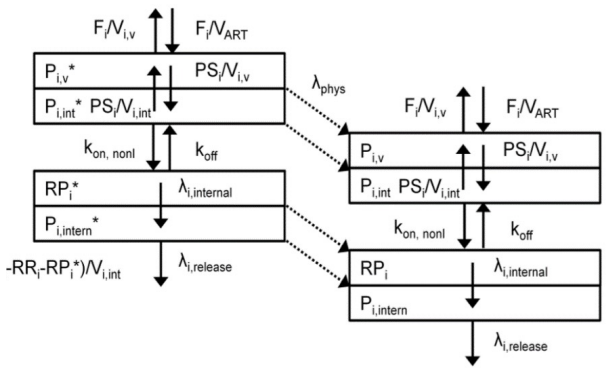


## Advantages of using the PBPK Model:

- Using a priori anatomical and physiological information
- Simultaneous analysis and fitting of all organs and tumors

## Study Workflow

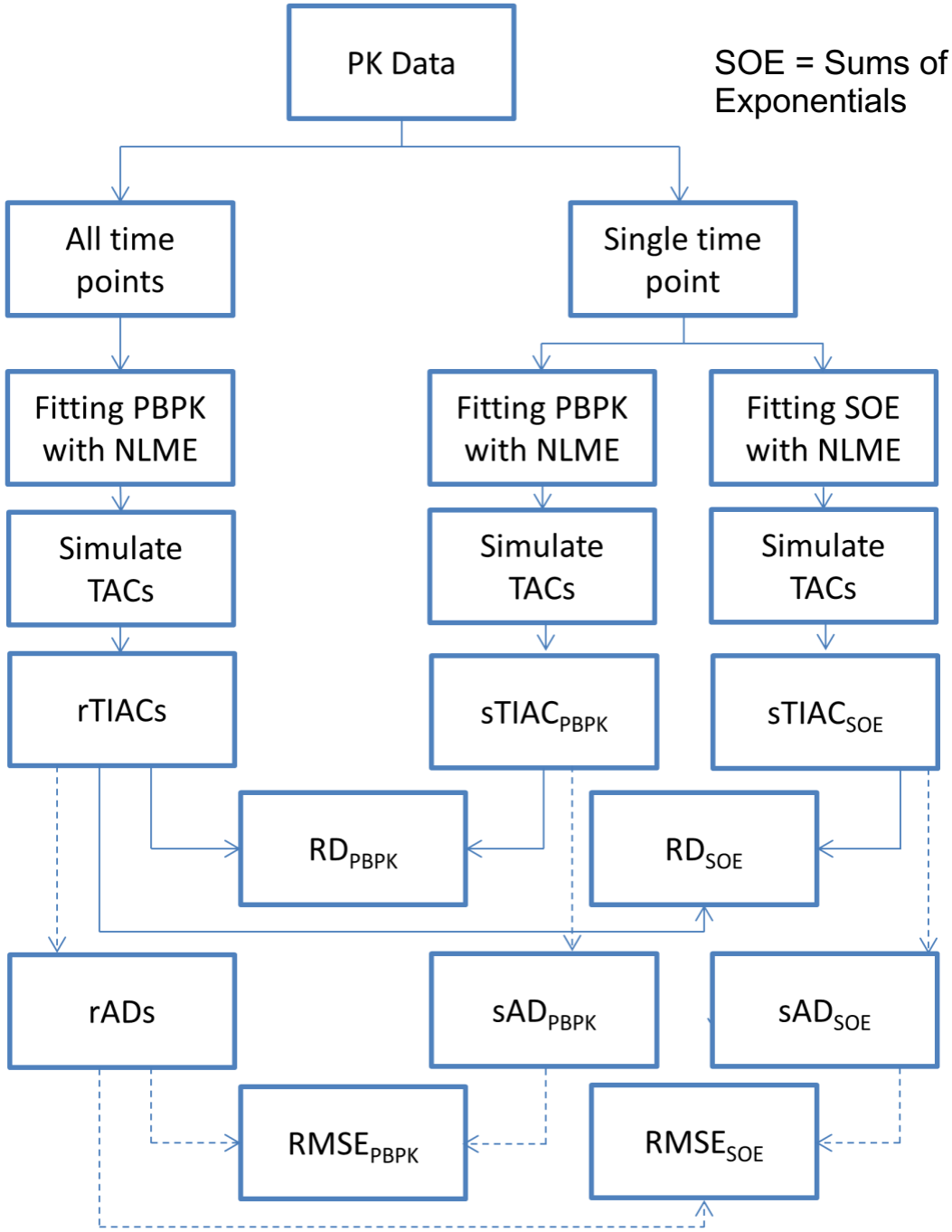

Presentation #2433, SS41

Tue, June 14 3:48-4:00 114/115

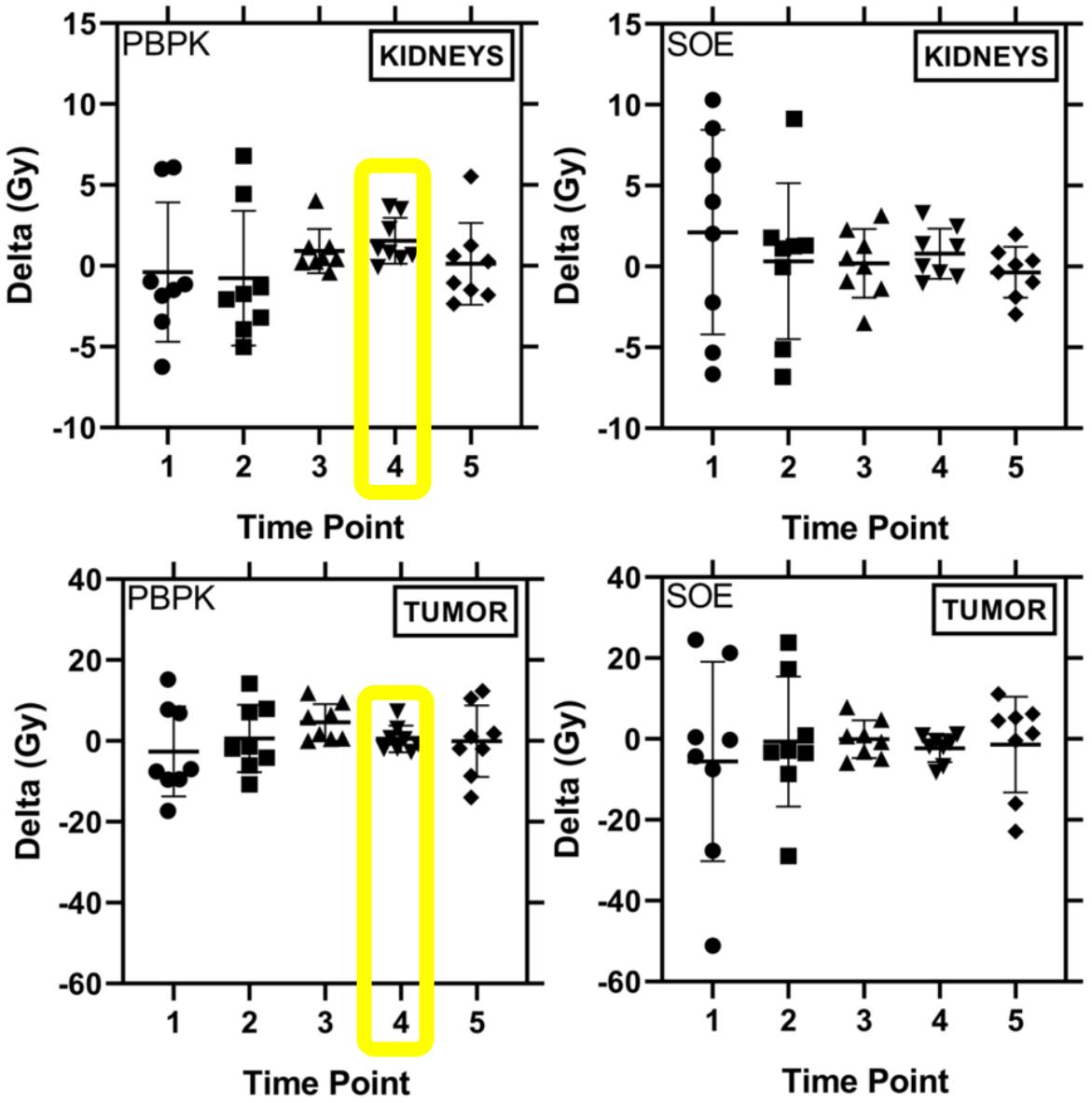


# Results and Conclusions

- investigated time points p.i.:
  - T1=(2.9±0.6) h
  - T2=(4.6±0.4) h
  - T3=(22.8±1.6) h
  - T4=(46.7±1.7) h
  - T5=(70.9±1.0) h
- T4 best (no diff. between PBPK and SOE)
- earlier time points: PBPK better

**Conclusion:** a single measurement at TP4=(46.7±1.7) h p.i. of $^{111}$In-DOTATATE might be used to predict individual TIACs/ADs of $^{90}$Y-DOTATATE in the kidneys and tumors in PRRT.

Presentation #3187, PIDS Poster

Sat, June 11 6:00-8:00 PM Hall A

# A Histology-based 3D Model of the Renal Cortical Labyrinth to Support Alpha-Particle Radiopharmaceutical Therapy


***B President[1], A Dozic[2], R Bolden II[1], L Ellis[3], C Colon-Ortiz[3], A Sforza[3], J Aris[4], G Sgouros[5], E Frey[6], R Hobbs[7], W Bolch[3]***

**1 Medical Physics Program, College of Medicine, University of Florida, Gainesville, FL 32611**
**2 Department of Physics, University of Florida, Gainesville, FL 32611**
**3 J. Crayton Pruitt Family Department of Biomedical Engineering, University of Florida, Gainesville, FL 32611**
**4 Department of Anatomy and Cell Biology, University of Florida, Gainesville, FL 32610**
**5 Department of Radiology, Johns Hopkins Medical Institutions, Baltimore, MD 21231**
**6 Radiopharmaceutical Imaging and Dosimetry, LLC, Baltimore, MD 21231**
**7 Department of Radiation Oncology, Johns Hopkins Medical Institutions, Baltimore, MD 21231**


Aim of the study: To develop a 3D histology-based model of the renal cortical labyrinth to support radiation dosimetry of alpha-particles (50–80 μm range) as needed for the development and clinical use of dose-response models of renal toxicity in RPT.

Presentation #3187, PIDS Poster

Sat, June 11 6:00-8:00 PM Hall A

# Methods

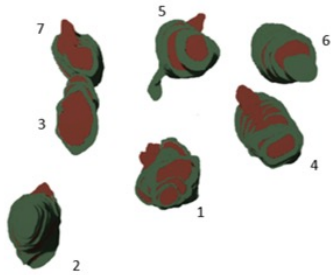


**1.** Exported segments from 3D Slicer into Rhinoceros 3D

| Glomerulus # | Diameter (Microns) |
|---|---|
| 1 | 177 |
| 2 | 218 |
| 3 | 210 |
| 4 | 202 |
| 5 | 213 |
| 6 | 225 |
| 7 | 250 |

**2b.** Table showing the maximum diameters measured in 3D Slicer.

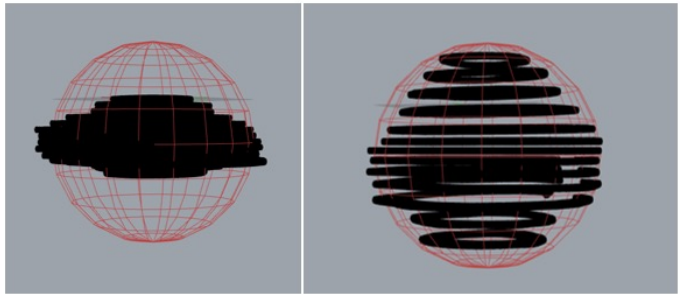

**2a.** Realigning slices of a renal corpuscle into a stylized sphere with a diameter that corresponds with the maximum diameter measured in 3D Slicer.

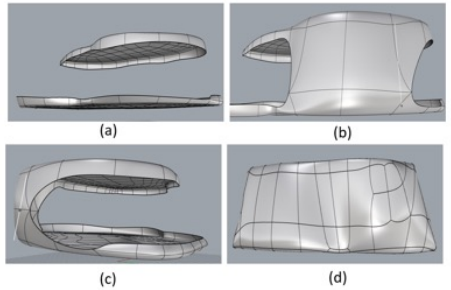


**2b.** Combining the slices to produce a continuous mesh.

Fig1: Steps for the Reconstruction of Renal Corpuscles

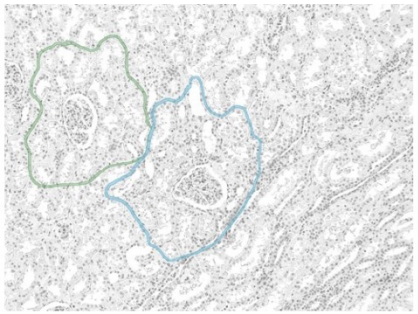

**A.** Border lines were drawn around each renal corpuscles to acquire all its respective tubules. (3D Slicer)

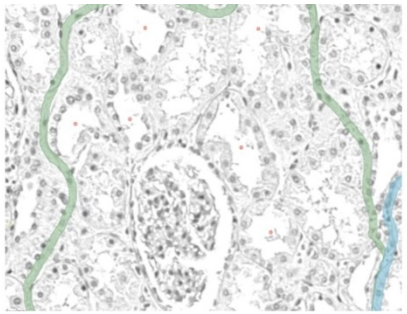

**B.** Points were drawn at the center of each tubule. (3D Slicer)

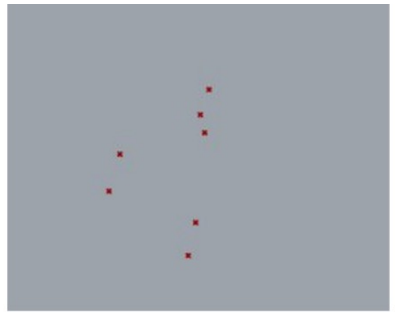

**C.** The points were realigned to show progression of the tubule in the z-direction. (Rhino 3D)

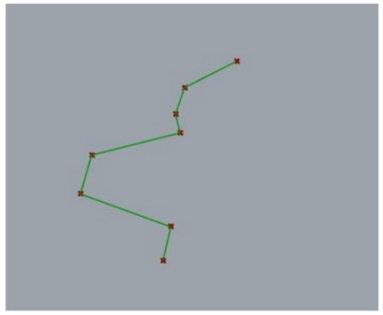

**D.** A polyline was generated to connect all tubular points. (Rhino 3D)

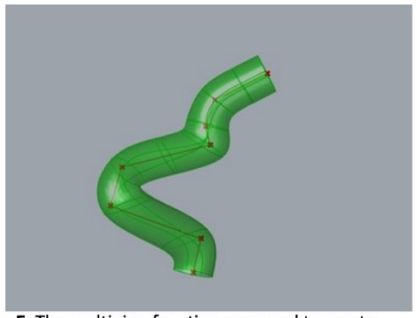

**E.** The multipipe function was used to create both the proximal and distal tubules at their respective diameters. (Rhino 3D)

Fig2: Steps for the Reconstruction of the Convoluted Tubules

Presentation #3187, PIDS Poster

Sat, June 11 6:00-8:00 PM Hall A

# Results and Conclusions

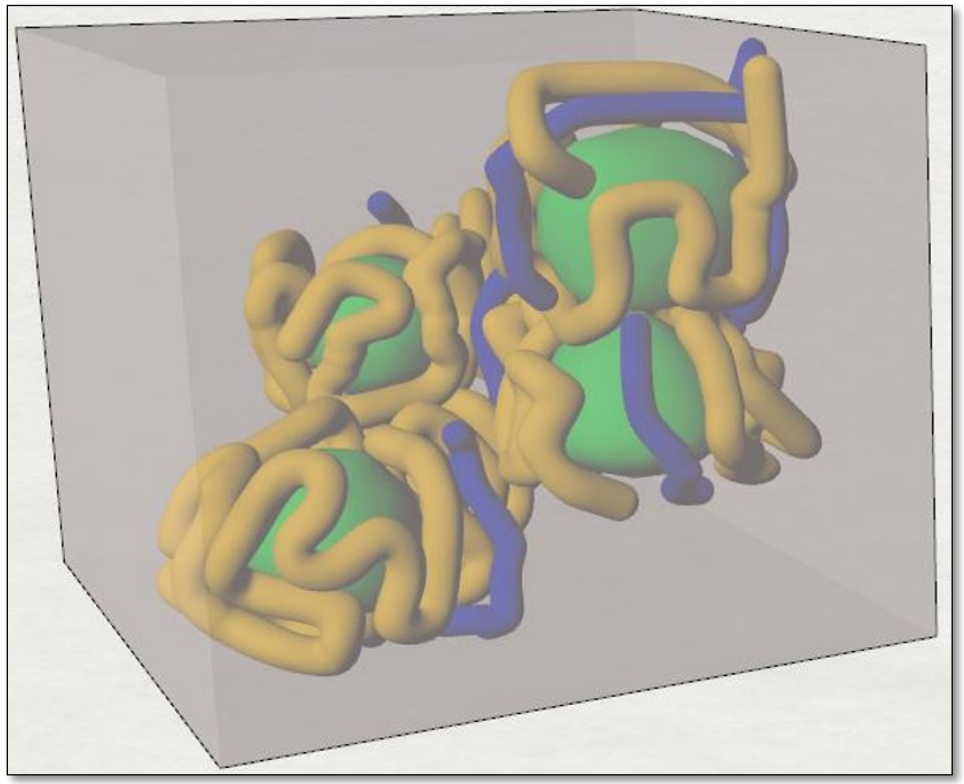

**Phase 1 Model:** Reconstructed Renal Corpuscles with their respective tubules.

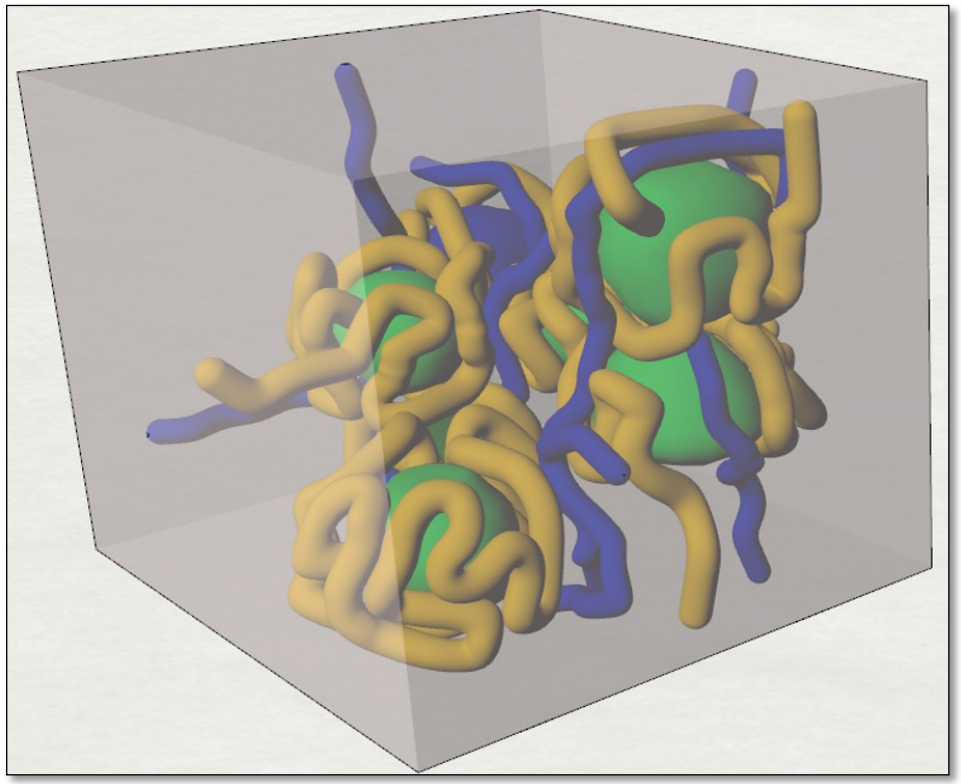

**Phase 2 Model:** Reconstructed Renal Corpuscles with their respective tubules extended to the borders of the 1mm$^3$ bounding box.

**Conclusion: A 3D model was successfully developed to include seven (7) Renal Corpuscles, the Proximal and Distal Convoluted Tubules.**

# Segmentation

Presentation #2413, SS30
Tue, June 14 9:12-9:24 109

Washington University in St. Louis
James McKelvey School of Engineering
Washington University in St. Louis
School of Medicine
MIR Mallinckrodt Institute of Radiology

# Need for objective task-based evaluation of segmentation methods in oncological PET: a study with ACRIN 6668/RTOG 0235 multi-center clinical trial data

Ziping Liu, Joyce C. Mhlanga, Barry A. Siegel, Abhinav K. Jha

Computational Medical Imaging Lab, Department of Biomedical Engineering, Mallinckrodt Institute of Radiology

**Aim of the study:**

**Investigate whether evaluation of PET segmentation methods using conventional figures of merit leads to similar inference as evaluation on clinical tasks**

Presentation #2413, SS30

Tue, June 14 9:12-9:24 109

Washington University in St. Louis
James McKelvey School of Engineering

Washington University in St. Louis
School of Medicine

MIR Mallinckrodt Institute of Radiology

# Methods

Evaluating segmentation methods using a **conventional figure of merit** (Dice score) and on the **clinical task of quantifying metabolic tumor volume (MTV)** of primary tumor

ACRIN 6668/RTOG 0235 multi-center clinical trial

FDG-PET images acquired pre-chemoradiotherapy

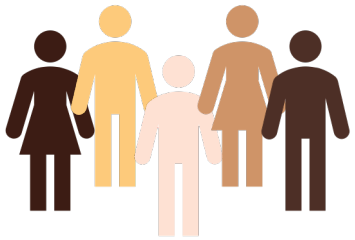

N = 225 patients with inoperable stage IIB/III NSCLC

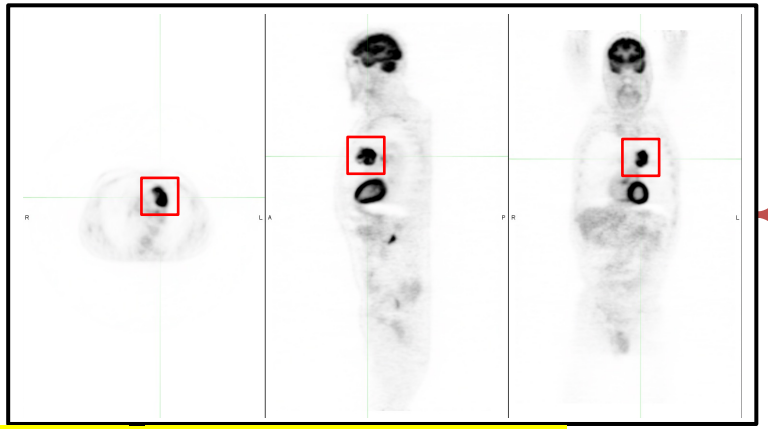

Ground-truth segmentation: primary tumor segmented by a board-certified nuclear-medicine physician (J.C.M)

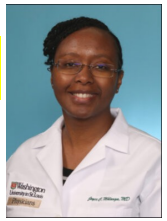

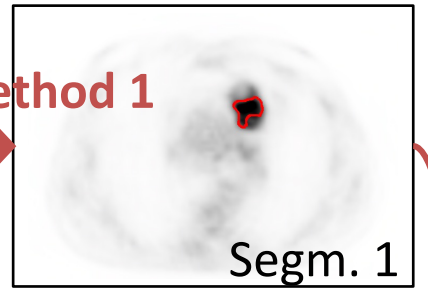


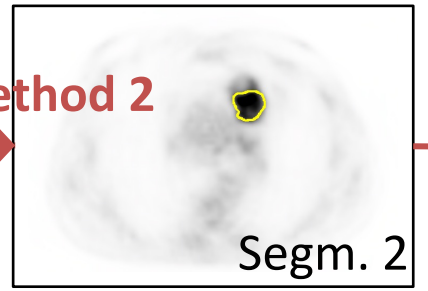


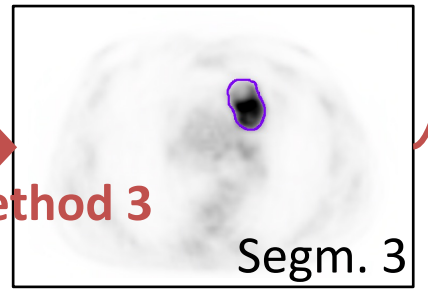


**Figures of merit to evaluate segmentation methods**

(a) Dice score

**(b) Task-specific: Ensemble normalized bias of estimated MTV**

Presentation #2413, SS30

Tue, June 14 9:12-9:24 109

Washington University in St. Louis
James McKelvey School of Engineering

Washington University in St. Louis
School of Medicine

MIR Mallinckrodt Institute of Radiology

# Results and conclusions

**Lower** Dice score **BUT more accurate** MTV quantification

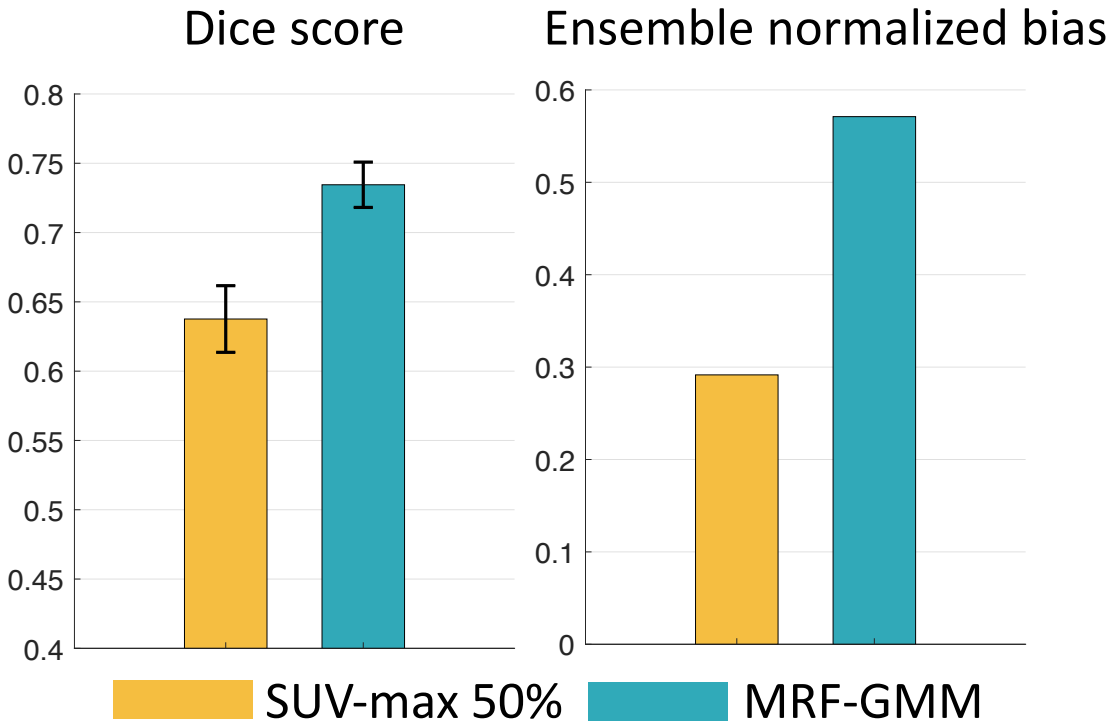


Deeper network yielded **similar** Dice score **BUT more accurate** MTV quantification

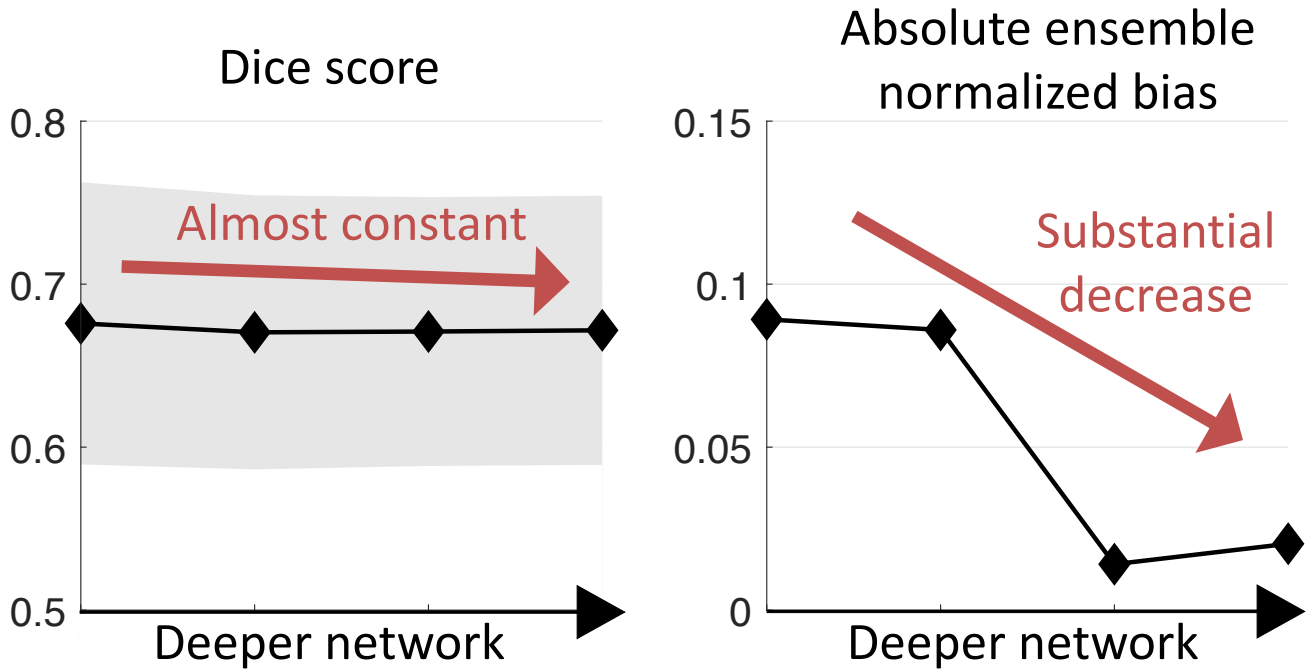


These results outlined the important **need for objective task-based evaluation** of oncological PET segmentation methods

Presentation #2410, SS30
Tue, June 14 8:36-8:48 109

# [18F]FDG-PET maximum intensity projections and artificial intelligence: a win-win combination to easily measure prognostic biomarkers in DLBCL patients

Kibrom B. Girum, Louis Rebaud, Anne-Ségolène Cottereau, Michel Meignan, Jérôme Clerc, Laetitia Vercellino, Olivier Casasnovas, Franck Morschhauser, Catherine Thieblemont, Irène Buvat

Aim of the study: *To investigate whether TMTV and Dmax features could be replaced by surrogate features automatically calculated using an artificial intelligence (AI) algorithm from only two maximum intensity projections (MIP) of the whole-body 18F-FDG PET images.*

Presentation #2410, SS30

Tue, June 14 8:36-8:48 109

# Methods

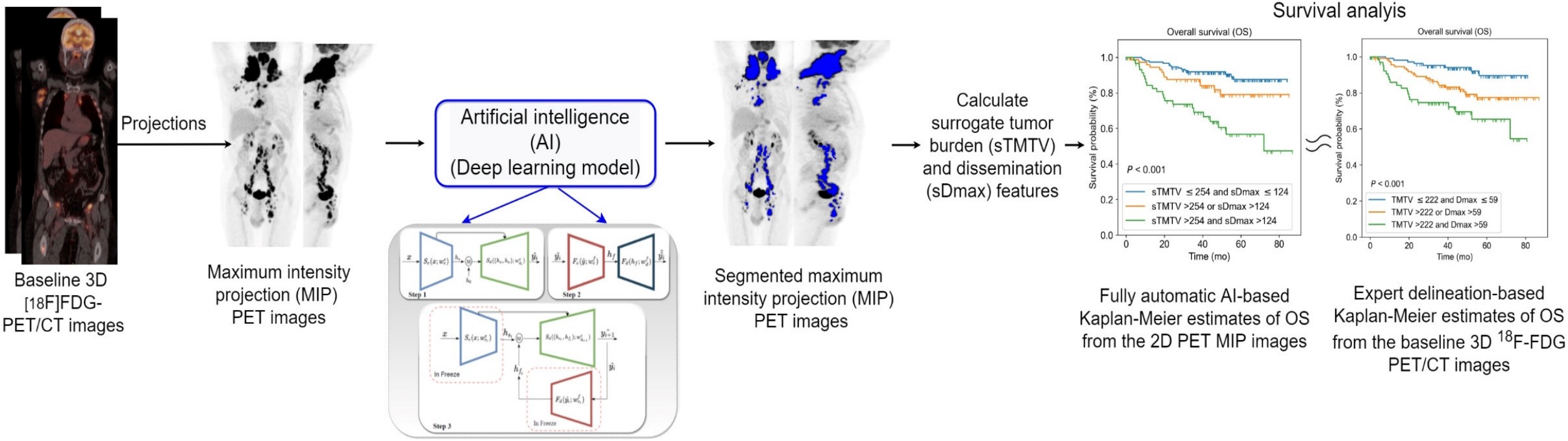


The AI was trained on an independent DLBCL patient and Tested on another independent cohort.

The code is publicly available: https://github.com/KibromBerihu/ai4elife

Presentation #2410, SS30

Tue, June 14 8:36-8:48 109

# Results and Conclusions

## Segmentation results

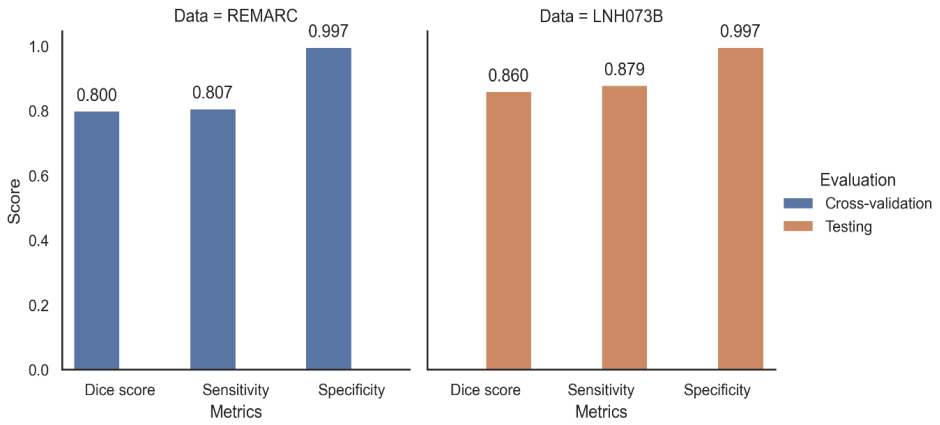


## Expert and AI-driven feature's correlation

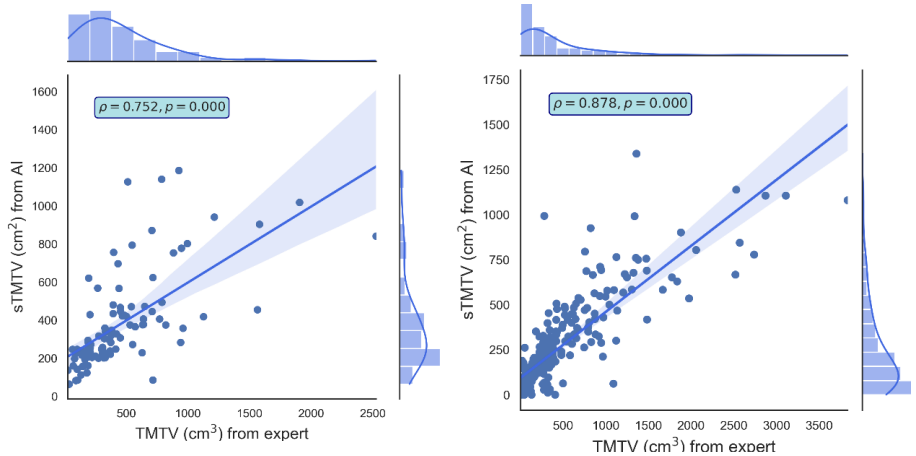


## Survival analysis

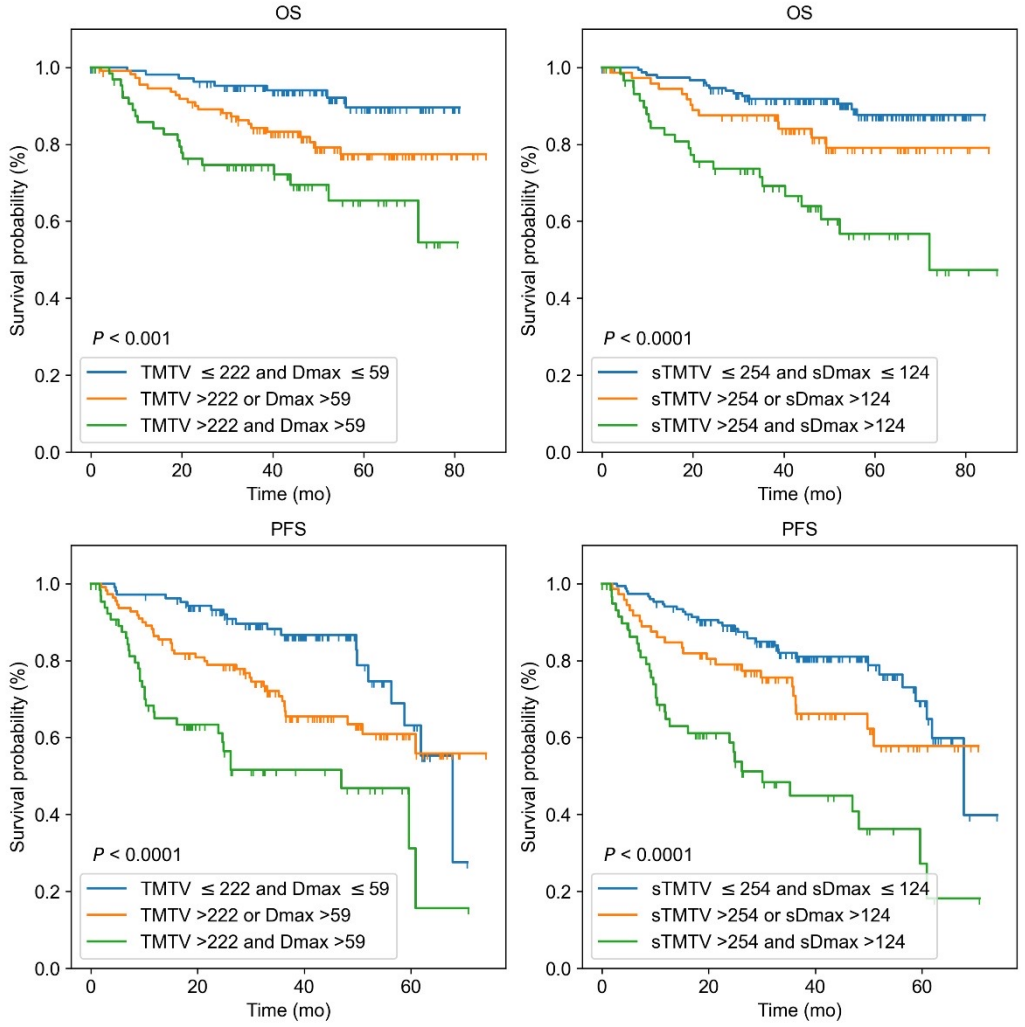


Conclusion: Surrogate TMTV and Dmax biomarkers automatically calculated using an AI algorithm from only 2 PET MIP images are prognostic biomarkers in DLBCL patients.

Presentation #2408, SS30
Tue, June 14 8:12-8:24 109

UMC Utrecht

# Automatic healthy liver segmentation for Holmium-166 radioembolization

**Stella M**, van Rooij R, Lam MGEH, de Jong HWAM and Braat AJAT

Department of Radiology and Nuclear Medicine, University Medical Center Utrecht, Utrecht (NL)

Aim of the study: to assess the automatic healthy liver segmentation using technetium-99m ($^{99m}$Tc) images derived from a dual isotope acquisition for holmium-166 dosimetry

Presentation #2408, SS30

Tue, June 14 8:12-8:24 109

# Methods

## Comparison of manual and automatic healthy liver segmentation for $^{166}$Ho dosimetry

34 procedures

### Current clinical practice

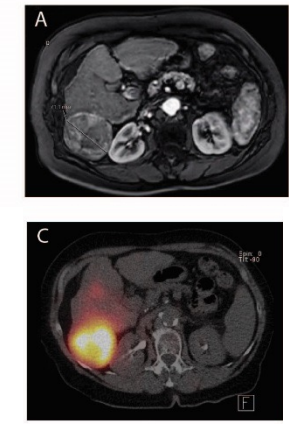


manual segmentation of
contrast enhanced CT
+
rigid registration of CT
on corresponding SPECT

### $^{166}$Ho-$^{99m}$Tc dual isotope protocol

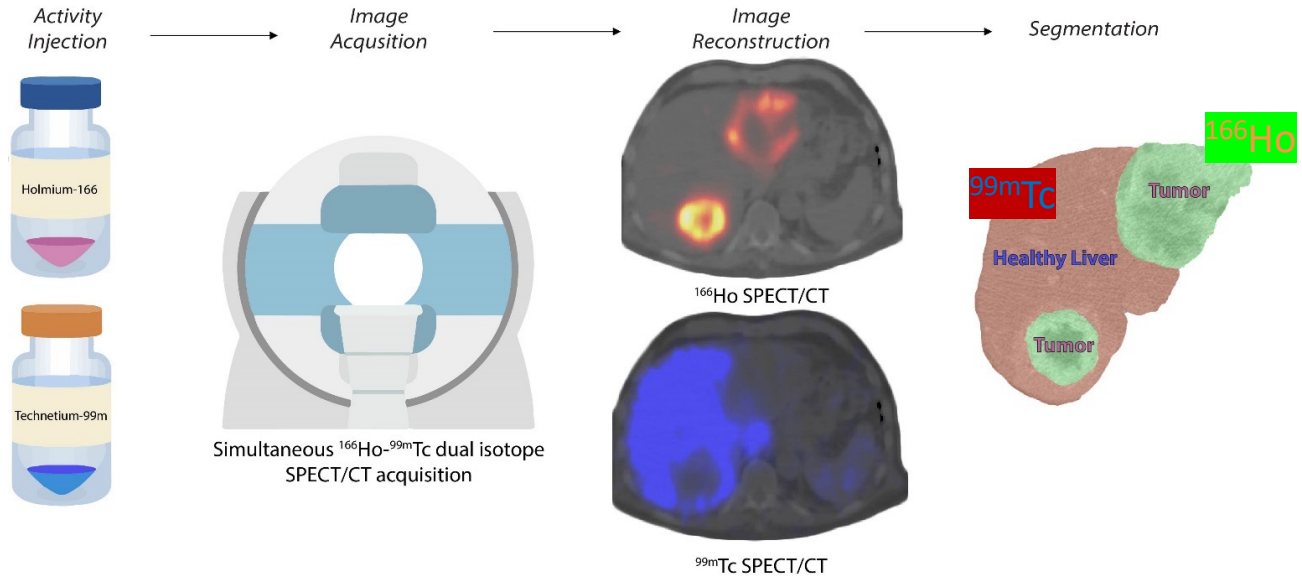

Presentation #2408, SS30

Tue, June 14 8:12-8:24 109

# Results and conclusions

| | | |
|---|---|---|
| |  |  |
|  | 36 ± 17 minutes | instantaneous |
|  Dose | 19 Gy ± 8 Gy | 21 Gy ± 9 Gy |

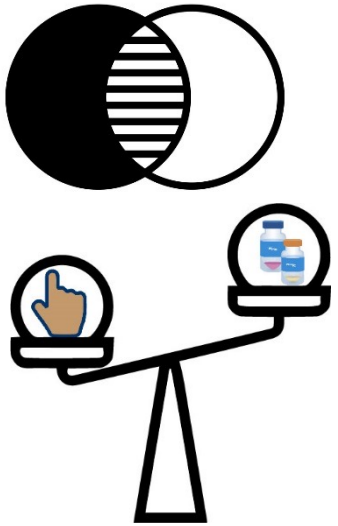

DICE: 0.8 ± 0.1

*Task-based* ☺

- 2 Gy ± 4 Gy (range -3 to + 8 Gy)
- p-value < 0.05

$^{166}$Ho-$^{99m}$Tc dual isotope protocol can be used to automatize the healthy liver segmentation without hampering the $^{166}$Ho dosimetry assessment

Presentation #2409, SS30
Tue, June 14 8:24-8:36 109

SIEMENS Healthineers

# Preliminary Evaluation of Lung Segment Parcellation for Lung Image Analysis

Fei Gao[1], Guenther Platsch[2], Zhoubing Xu[3], Dominik Neumann[2], Sasa Grbic[3], Bruce Spottiswoode[1]

[1] Siemens Medical Solutions USA, Inc., Knoxville, TN, USA
[2] Siemens Healthcare GmbH, Erlangen, Germany
[3] Siemens Medical Solutions USA, Inc., Princeton, NJ, USA

**Study Aim**: The lung segment is considered the minimum functional/operable unit. However, anatomical boundaries are not clearly visible and accurate demarcation of the segments requires meticulous navigation on the CT referencing bronchi and pulmonary vessel pathways. This work comprises a preliminary evaluation of a newly developed deep learning-based lung segment parcellation workflow for SPECT/CT and PET/CT.

Presentation #2409, SS30

Tue, June 14 8:24-8:36 109

# Methods

SIEMENS Healthineers

## Annotation:

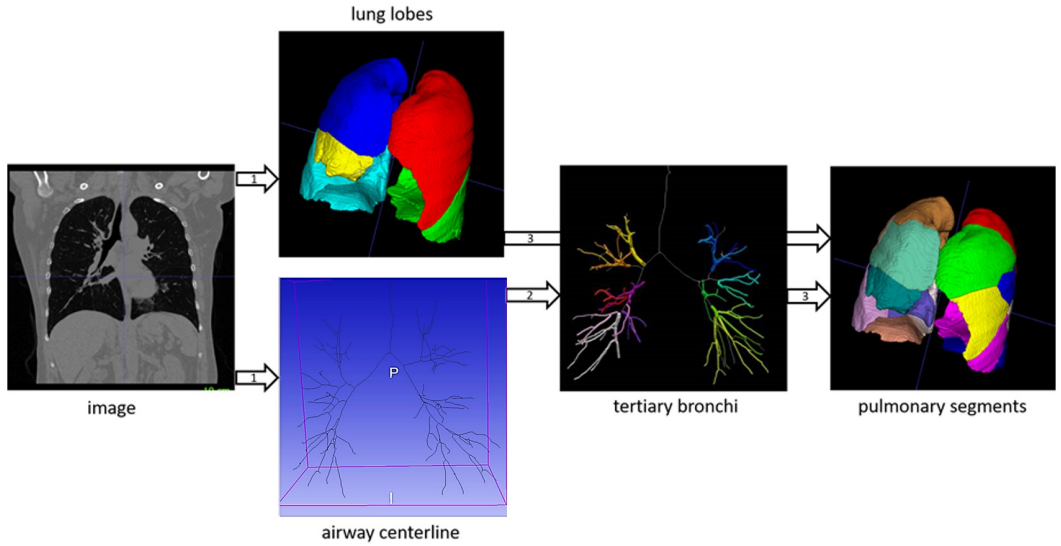


## Algorithm implementation:

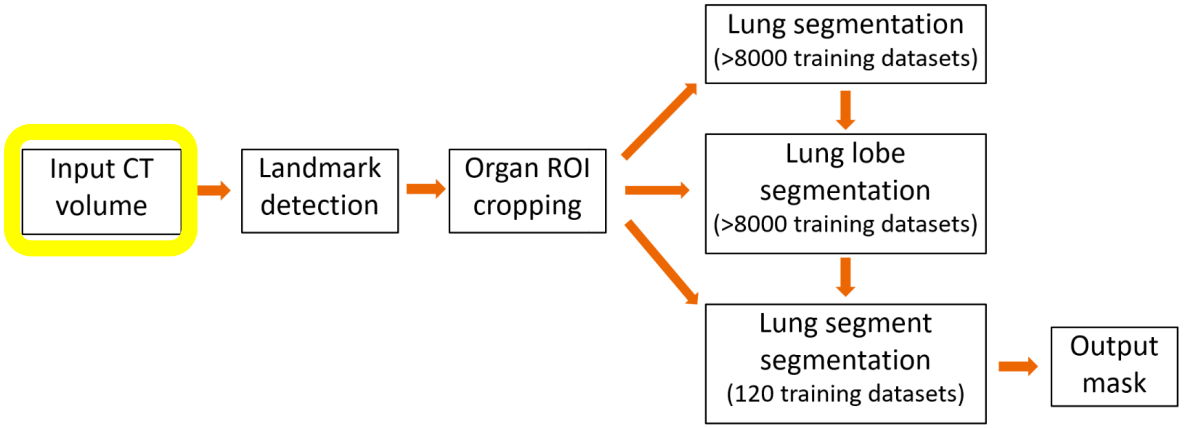


## Evaluation:

Quantitative metrics as well as qualitative anatomical evaluation by a board-certified nuclear medicine physician.

Presentation #2409, SS30

Tue, June 14 8:24-8:36 109

# Results and Conclusions

## Qualitative evaluation by NM expert

(13 cases, both normal and abnormal lungs)

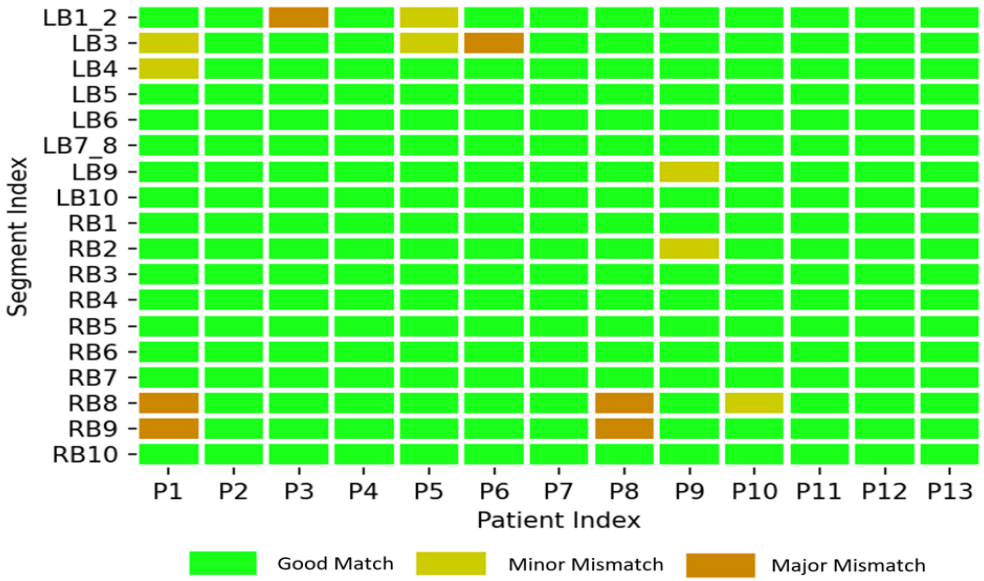


LB1_2: Left Apical Posterior; LB3: Left Anterior; LB4: Left Superior Lingula; LB5: Left Inferior Lingula; LB6: Left Superior; LB7_8: Left Anteriomedian Basal; LB9: Left Lateral Basal; LB10: Left Posterior Basal; RB1: Right Apical; RB2: Right Posterior; RB3: Right Anterior; RB4: Right Lateral; RB5: Right Medial; RB6: Right Superior; RB7: Right Medial Basal; RB8: Right Anterior Basal;RB9: Right Lateral Basal; RB10: Right Posterior Basal

## Illustrative case

(demonstrating additional clinical benefit of lung segment parcellation to support resection planning using a lung perfusion SPECT/CT scan)

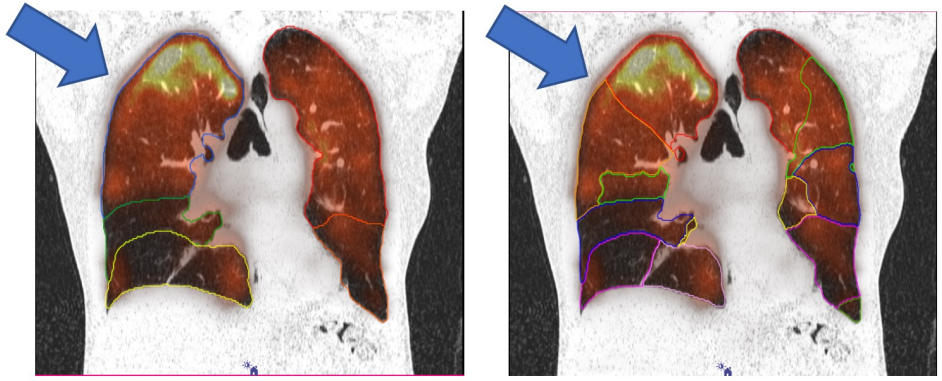

**Conclusion**: this preliminary evaluation yielded encouraging results for the potential clinical usage of lung analysis at the pulmonary segment level.

Presentation #2518, SS30

Tue, June 14 8:00-8:12 109

THE UNIVERSITY OF TEXAS MD Anderson Cancer Center | UTHealth The University of Texas Health Science Center at Houston

Graduate School of Biomedical Sciences

# Functional Tumor Diameter Measurement with Molecular Breast Imaging (MBI)

**Benjamin P. Lopez [1]**,
Gaiane M. Rauch [2], Beatriz Adrada [2], S. Cheenu Kappadath[1]

1. Department of Imaging Physics, UT MD Anderson Cancer Center, Houston, TX, USA
2. Department of Abdominal Imaging, UT MD Anderson Cancer Center, Houston, TX, USA

## Aim of Study:

To absolutely quantify focal breast lesion diameters using standard-of-care patient imaging on a commercially-available Molecular Breast Imaging system

## Related Work: Poster #3256

Absolute $^{99m}$Tc tumor activity uptake quantification with Molecular Breast Imaging

Presentation #2518, SS30
Tue, June 14 8:00-8:12 109

# Methods

THE UNIVERSITY OF TEXAS MD Anderson Cancer Center | UTHealth The University of Texas Health Science Center at Houston
Graduate School of Biomedical Sciences

## Development and Testing in Monte Carlo Simulations

- Validation of GE Discovery NM750b in Lopez, *PMB*, 2021
- Training and testing performed on >75,000 unique conditions

### Key Finding

Simple linear equation accurately (<1 pixel-width) estimated diameter from tumor profile FWHM on image

$$d^{MBI} = 1.2\ mm + 1.2 \times FWHM$$

## Semi-Automatic Implementation in 64 Patient Data Set

- Patients with locally-advanced cancer pre-neoadjuvant chemotherapy (NCT02324387)
- Longest tumor diameters calculated:
  - Proposed MBI methodology ($d^{MBI}$)
  - Physician MBI tumor contours ($d^{ROI}$)
  - Physician mammography measurement ($d^{MG}$)
  - Physician ultrasound measurement ($d^{US}$)
- Evaluation of semi-automatic methodology
  - Success rate in estimating diameter
  - Absolute difference with physician values

Presentation #2518, SS30

Tue, June 14 8:00-8:12 109

# Results and Conclusions

THE UNIVERSITY OF TEXAS MD Anderson Cancer Center | UTHealth The University of Texas Health Science Center at Houston

Graduate School of Biomedical Sciences

**Semi-automatically calculated longest diameters ($d^{MBI}$) were**

Successfully estimated in 94% of patients (60/64) and

Mostly within ±5 mm of physician MBI ($d^{ROI}$), MG, and US measurements

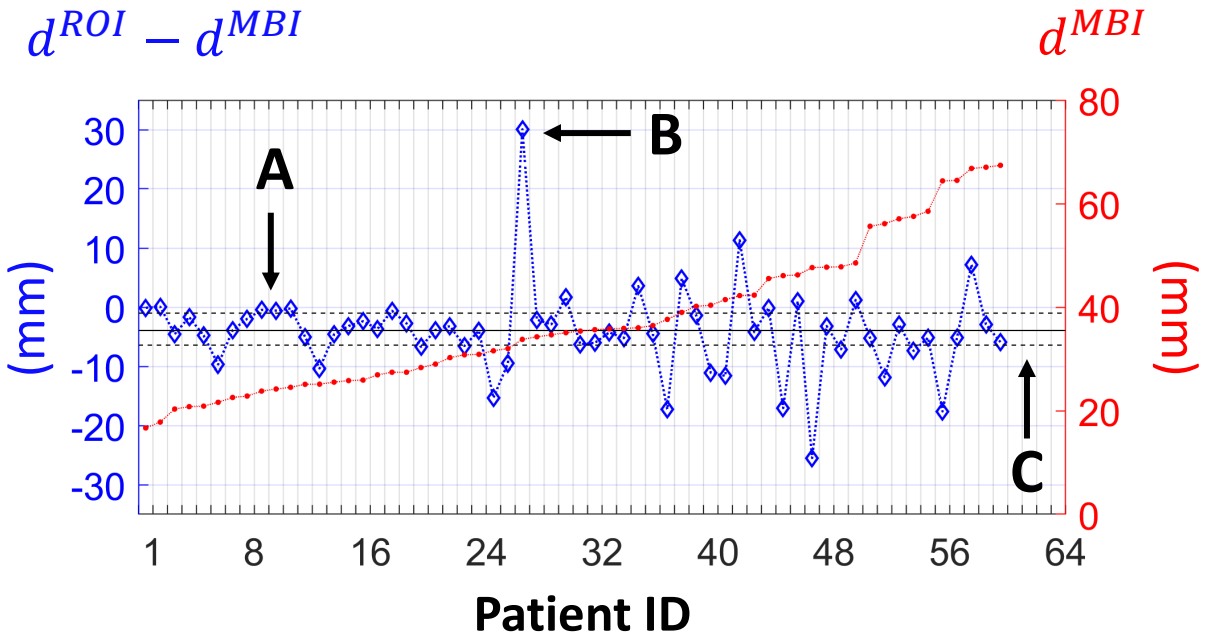


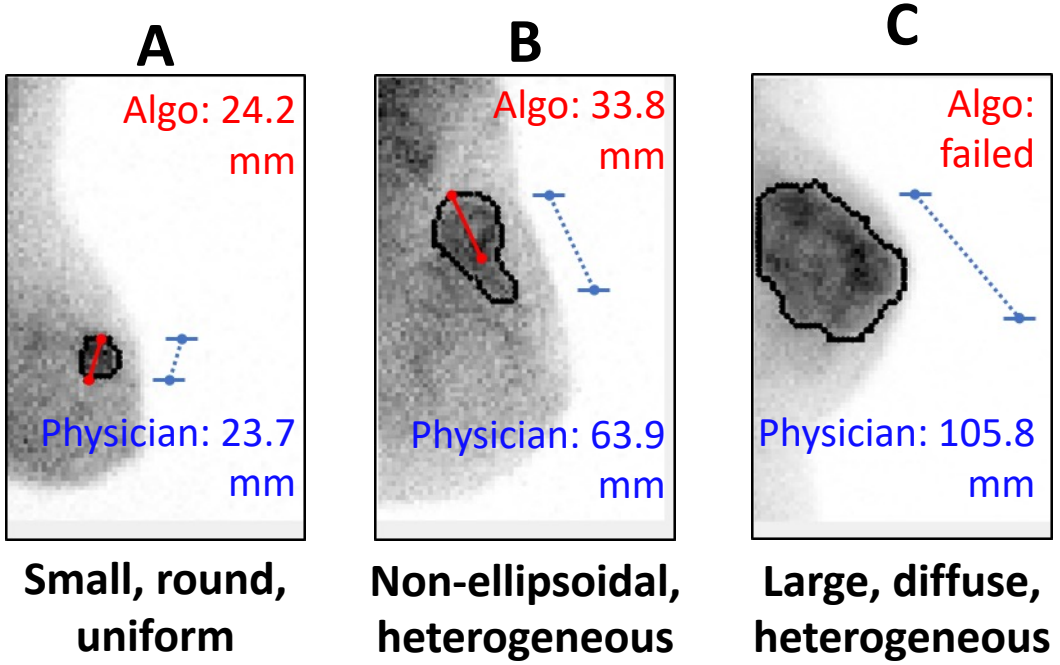


**Small, round, uniform**

**Non-ellipsoidal, heterogeneous**

**Large, diffuse, heterogeneous**

**First-ever large patient cohort study demonstrates the feasiblity and challenges of accurate and reliable functional tumor size quantitation with clinical MBI imaging**


June 11-14
2022
SNMMI ANNUAL MEETING
Vancouver, British Columbia, Canada

# Radiomics

Presentation #3168, PIDS Poster

Sat, June 11 6:00-8:00 PM Hall A

# Prediction of Lymphovascular Invasion in Non-Small Cell Lung Carcinoma Using Multimodality PET/CT Fusion Radiomics

Mehdi Amini[1], Ghasem Hajianfar[2], Isaac Shiri[1], Habib Zaidi[1,3,4,5]

[1]Division of Nuclear Medicine and Molecular Imaging, Geneva University Hospital, Geneva, Switzerland
[2]Rajaie Cardiovascular Medical and Research Center, Iran University of Medical Science, Tehran, Iran
[3]Geneva University Neurocenter, University of Geneva, 1205 Geneva, Switzerland
[4]Department of Nuclear Medicine and Molecular Imaging, University of Groningen, Groningen, Netherlands
[5]Department of Nuclear, University of Southern Denmark, Odense, Denmark

Aim of the study: Prediction of Lymphovascular Invasion in Non-Small Cell Lung Carcinoma using single- and multi-modality PET/CT fused radiomics models, trained by various feature selection (FS) and machine learning (ML) methods.

Presentation #3168, PIDS Poster

Sat, June 11 6:00-8:00 PM Hall A

# Methods

*heavily unbalanced !*

- Cohort -> 146 NSCLC patients (126 LVI positive, 20 LVI negative); divided to 70-30% partitions for training/validating and testing cohorts.
- Tumor segmentation -> on CT scans by an experienced radiologist.
- PET and CT image fusion -> (1) Guided Filtering Fusion, (2) Weighted Least Square.
- Radiomics extraction -> SERA package (based on IBSI guidelines); Features -> Morphological, intensity based, and textural.
- Feature selection methods -> (1) Boruta, (2) Maximum Relevance Minimum Redundancy, and (3) (RFE)
- Machine Learning algorithms -> (1) DT, (2) KNN, (3) LR, (4) MLP, (5) NB, (6) RF, (7) SVM, (8) XGB
- Performance evaluation -> area under ROC curve (AUC), accuracy (ACC), Sensitivity (SEN), and Specificity (SPE).

CT PET GFF WLS

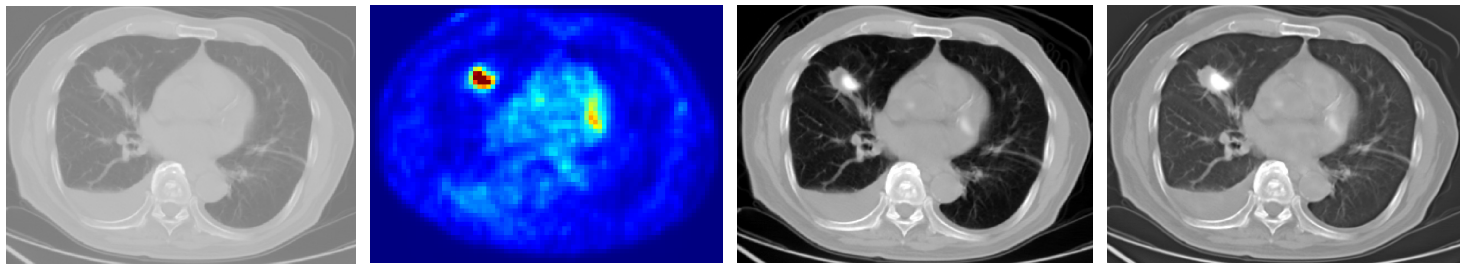

Presentation #3168, PIDS Poster

Sat, June 11 6:00-8:00 PM Hall A

Hôpitaux Universitaires Genève

PINLab

# Results and Conclusions

| | Modality | Feature Selection | Machine Learning | AUC | ACC | SEN | SPE | *balanced ACC* |
|---|---|---|---|---|---|---|---|---|
| | CT | RFE | KNN | 0.81 | 0.72 | 0.84 | 0.71 | 0.77 ± ??? |
| | PET | Boruta | KNN | 0.80 | 0.75 | 0.83 | 0.73 | 0.78 |
| *PET+CT* | GFF | MRMR | LR | 0.81 | 0.70 | 0.84 | 0.68 | 0.76 |
| *PET+CT* | WLS | RFE | KNN | 0.78 | 0.75 | 0.67 | 0.76 | 0.71 |

- NSCLC Lymphovascular invasion can be predicted non-invasively by single- and multimodality PET/CT radiomics modeling.
- Radiomic features extracted from Multimodality fused images can better characterize tumor heterogeneities, since they reflect both anatomical (CT) and metabolic (PET) aspects of tumor, simultaneously.
- There is no fit to all algorithm, and different modalities achieved their best performance while trained by different combination of FS and ML algorithms.

*???*

Presentation #3167, PIDS Poster

Sat, June 11 6:00-8:00 PM Hall A

# [$^{68}$Ga]DOTATOC PET/CT radiomics in the prediction of response in GEP-NETs undergoing [$^{177}$Lu]DOTATOC PRRT: the "Theragnomics" concept


Riccardo Laudicella[1,2,3,4], Albert Comelli[2], Virginia Liberini[5,6], Antonio Vento[1], Alessandro Stefano[7], Alessandro Spataro[1], Ludovica Crocè[1], Sara Baldari[8], Michelangelo Bambaci[9], Desiree Deandreis[5], Demetrio Arico'[9], Massimo Ippolito[8], Michele Gaeta[10], Pierpaolo Alongi[4], Fabio Minutoli[1], Irene A. Burger[3,11] and Sergio Baldari[1]

**1.** Nuclear Medicine Unit, Department of Biomedical and Dental Sciences and Morpho-Functional Imaging, University of Messina, Italy; **2.** Ri.MED Foundation, Palermo, Italy; **3.** Department of Nuclear Medicine, University Hospital Zürich, Switzerland; **4.** Nuclear Medicine Unit, Fondazione Istituto G.Giglio, Cefalù, Italy; **5.** Nuclear Medicine Unit, Department of Medical Sciences, University of Turin, Italy; **6.** Nuclear Medicine Department, S. Croce e Carle Hospital, Cuneo, Italy; **7.** Institute of Molecular Bioimaging and Physiology, National Research Council (IBFM-CNR), Cefalù, Italy; **8.** Nuclear Medicine Department, Cannizzaro Hospital, Catania, Italy; **9.** Department of Nuclear Medicine, Humanitas Oncological Centre of Catania, Italy; **10.** Section of Radiological Sciences, Department of Biomedical Sciences and Morphological and Functional Imaging, University of Messina, Italy; **11.** Department of Nuclear Medicine, Kantonsspital Baden, Switzerland


**Aim** → To develop a new radiomics and ML predictive model of response to complete PRRT in GEP-NET patients analyzing [$^{68}$Ga]DOTA-PET/CT images.

Presentation #3167, PIDS Poster

Sat, June 11 6:00-8:00 PM Hall A

# Methods

Retrospective analysis of 38 GEP-NETs (**9 GI – 27 GII – 2 GIII**) underwent restaging [$^{68}$Ga]DOTA PET/CT on the same scanner within 2 months before and after complete PRRT

**324** SSTR-positive lesions (191 parenchymal, 42 bone, 91 lymph nodal)

[$^{177}$Lu]DOTATOC PRRT (5-7 cycles)

Mean dose 29.1GBq - Mean age 59.5y (35-79y)

Minimum follow-up after PRRT of 6 months (clinical, laboratory and imaging according to molecular imaging; mean FU = 8.7 months)

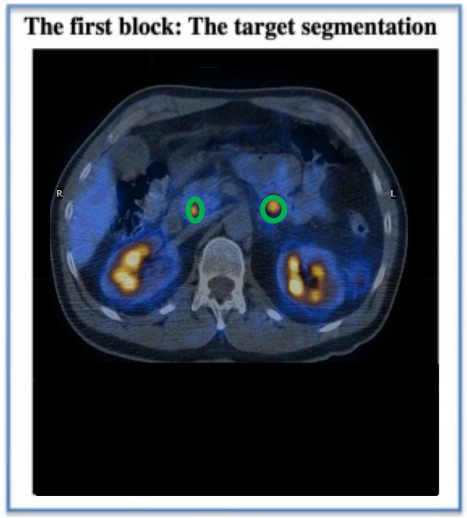


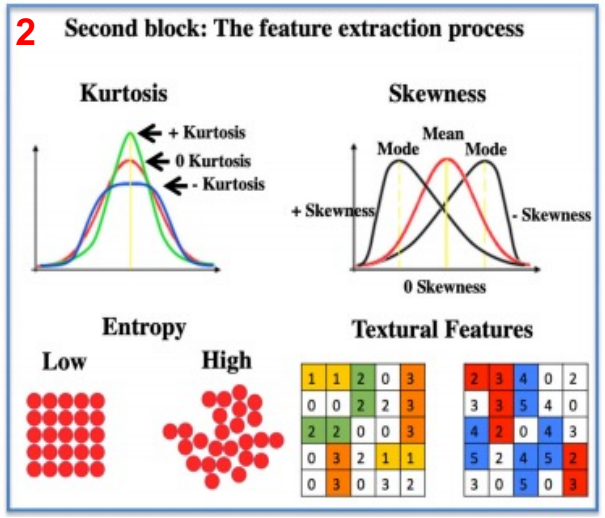


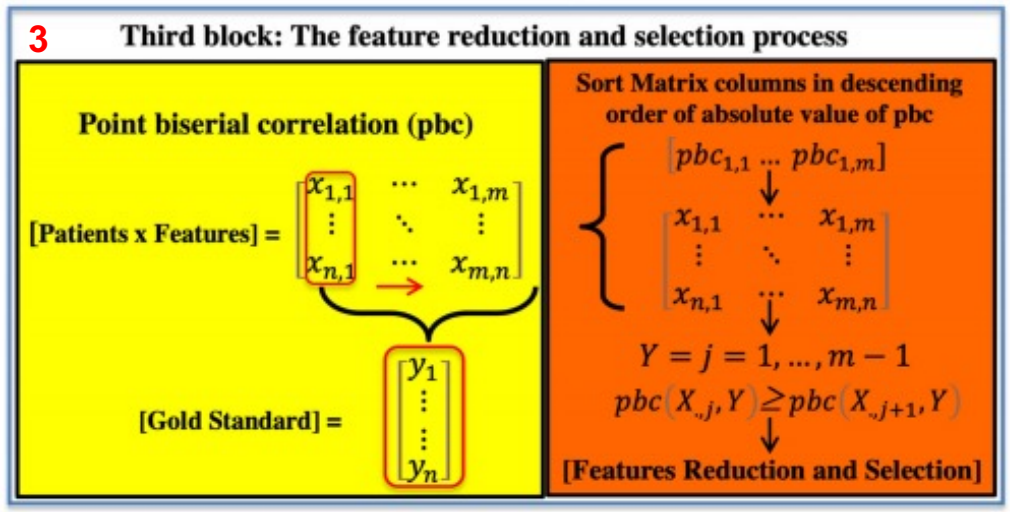


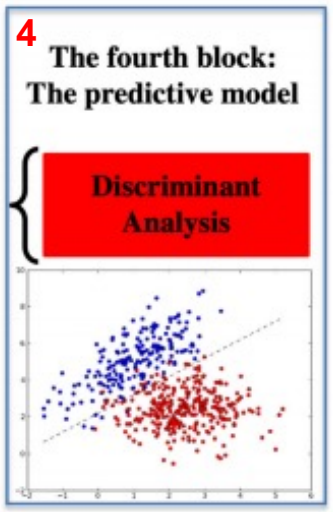

Presentation #3167, PIDS Poster

Sat, June 11 6:00-8:00 PM Hall A

# Results and Conclusions

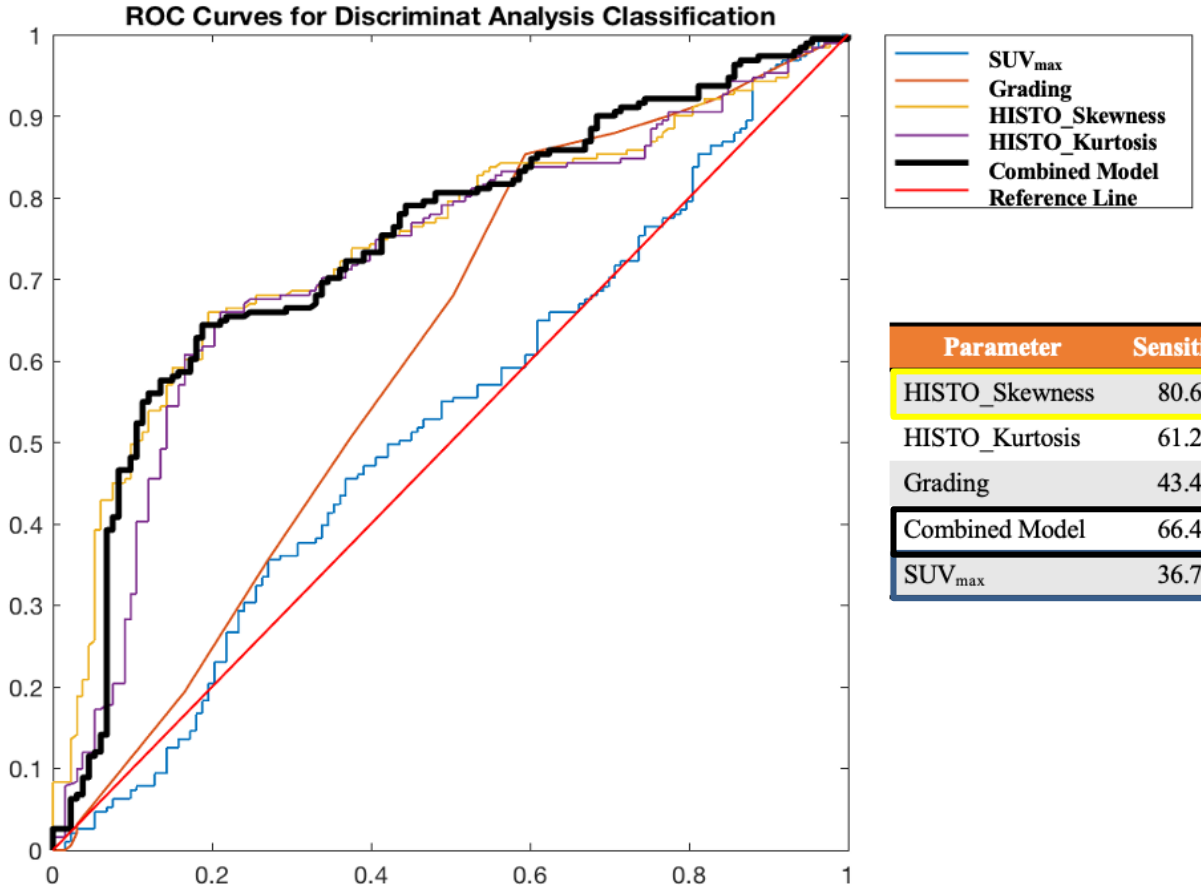


133 progressive lesions, 191 responding

| Parameter | Sensitivity | Specificity | AUC | p-value | cut-off | balanced ACC |
|---|---|---|---|---|---|---|
| HISTO_Skewness | 80.6% | 67.2% | 0.745 | < 0.001 | 2.5 | 74% ± ??? |
| HISTO_Kurtosis | 61.2% | 75.9% | 0.722 | < 0.001 | 6.9 | 69% |
| Grading | 43.4% | 83.7% | 0.609 | 0.004 | | 64% |
| Combined Model | 66.4% | 70.3% | 0.744 | < 0.001 | | 68% |
| $SUV_{max}$ | 36.7% | 63.3% | 0.523 | 0.49 | | 50% |

The presented exploratory theragnomics model proved to be **superior to conventional quantitative parameters to predict the response** of GEP-NET lesions in patients treated with complete [$^{177}$Lu]DOTATOC PRRT, regardless of the lesions' site. The opportunity to assess for each patient the **single lesion's heterogeneity** and predict each lesion's response to PRRT would enhance physicians to early address patients to the best options of care, reducing costs and potential toxicities (**Tailored Medicine)**

Presentation #1339, PIDS Poster

Sat, June 11 6:00-8:00 PM Hall A

# Effect of harmonization and oversampling methods on multi-center imbalanced PET datasets: Application to radiomics-based NSCLC-subtype prediction

***Dongyang Du***[1,2], *Isaac Shiri*[3], *Fereshteh Yousefirizi*[2], *Habib Zaidi*[3], *Lijun Lu*[1], *Arman Rahmim*[2]

1. School of Biomedical Engineering and Guangdong Provincial Key Laboratory of Medical Image Processing, Southern Medical University, Guangzhou, China.
2. Department of Integrative Oncology, BC Cancer Research Institute, Vancouver, Canada.
3. Division of Nuclear Medicine and Molecular Imaging, Geneva University Hospital, CH-1211 Geneva 4, Switzerland

Aim of the study: **to investigate the impact of harmonization and oversampling methods on multi-center imbalanced datasets in PET**, with specific application to radiomics-based predictive modeling of histologic subtype of non-small cell lung cancer (NSCLC).

Presentation #1339, PIDS Poster

Sat, June 11 6:00-8:00 PM Hall A

# Methods

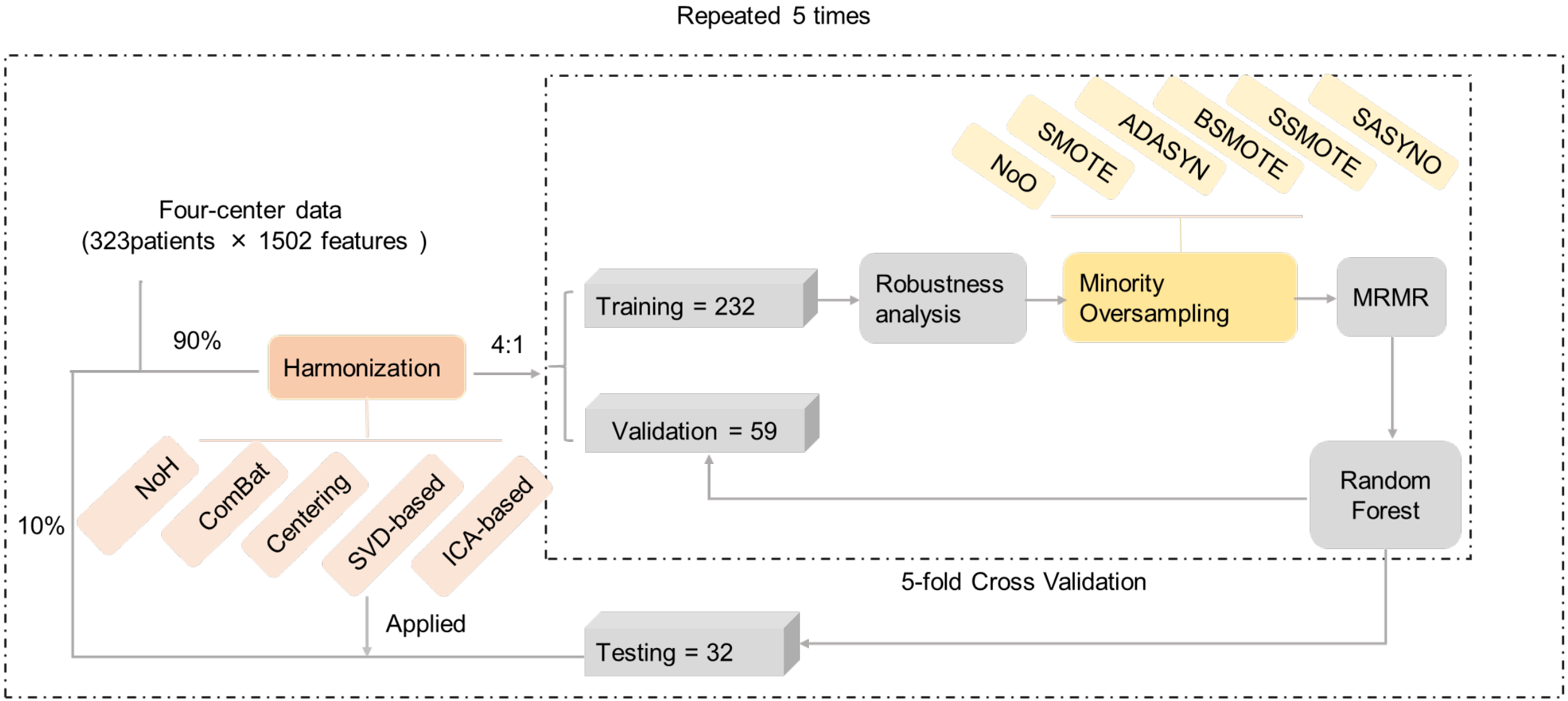

Presentation #1339, PIDS Poster

Sat, June 11 6:00-8:00 PM Hall A

# Results and Conclusions

**Table 3.** The performance comparisons between representative high-performing combinations and the baseline.

| Model | Internal validation | | | External testing | | |
|---|---|---|---|---|---|---|
| | AUROC | G-mean | p | AUROC | G-mean | p |
| NoH+NoO | 0.608 ± 0.058 | 0.398 ± 0.161 | | 0.567 ± 0.120 | 0.234 ± 0.224 | |
| NoH+SMOTE | 0.658 ± 0.082 | 0.573 ± 0.093 | * | 0.590 ± 0.109 | 0.418 ± 0.176 | * |
| ComBat+NoO | 0.696 ± 0.073 | 0.486 ± 0.136 | * | 0.661 ± 0.122 | 0.274 ± 0.203 | * |
| ComBat+SMOTE | 0.725 ± 0.079 | 0.625 ± 0.101 | * | 0.637 ± 0.117 | 0.363 ± 0.215 | * |
| ComBatCovar+NoO | 0.968 ± 0.022 | 0.848 ± 0.072 | *** | 0.663 ± 0.096 | 0.207 ± 0.214 | * |
| ComBatCovar+SMOTE | 0.969 ± 0.016 | 0.863 ± 0.061 | *** | 0.627 ± 0.096 | 0.307 ± 0.218 | * |

**Conclusion:** Harmonization and oversampling methods had a positive effect on NSCLC-subtype prediction in multi-center imbalanced PET radiomics analysis, but lack of generalization ability.

Presentation #2411, SS30

Tue, June 14 8:48-9:00 109

# Independent assessment of a recently identified PET biomarker and of IBSI-defined radiomic features to predict overall survival of lung cancer patients

Vesna Cuplov[1], Marie Luporsi[1,2], Christophe Nioche[1], Nina Jehanno[1,2], Hervé Brisse[1,3], Alain Livartowski[4], Nicolas Girard[4], Irène Buvat[1], Fanny Orlhac[1]

1: LITO, U1288 Inserm/Institut Curie, Orsay, France. 2: Institut Curie, Dpt of Nuclear Medicine, Paris, France.
3: Institut Curie, Dpt of Radiology, Paris, France. 4: Institut Curie, Institut du Thorax Curie-Montsouris, Paris, France.

Aim of the study: to assess the prognostic value of new PET biomarkers using an independent cohort of patients with advanced lung cancer.

Presentation #2411, SS30
Tue, June 14 8:48-9:00 109

# Methods

- 77 patients with advanced non-small cell lung cancer
- Baseline FDG-PET/CT: segmentation of primitive lesion only

## New PET biomarkers

**NHOC**: Normalized distance between **SUVmax** and the tumor **centroid** [Jimenez-Sanchez et al. *PNAS* 2021]

**NCoMS**: Normalized distance between the **intensity-weighted centroid** and the tumor **centroid**

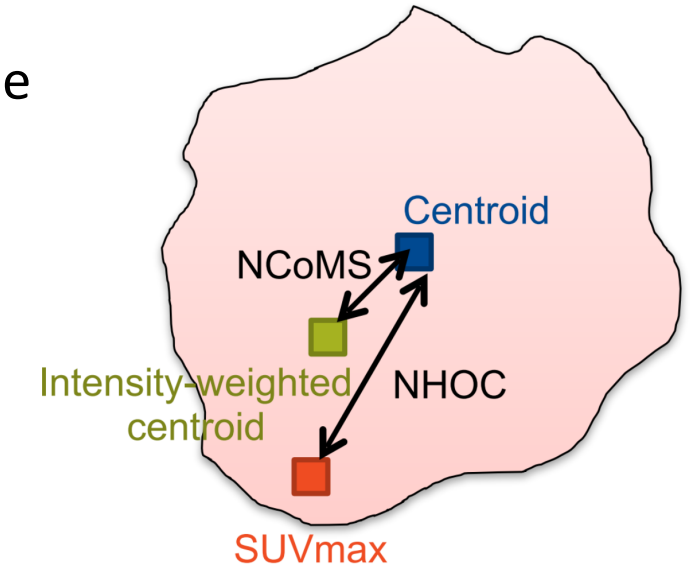

Presentation #2411, SS30

Tue, June 14 8:48-9:00 109

# Results and Conclusions

## Validation of NHOC prognostic value

**Our cohort (77 patients)**

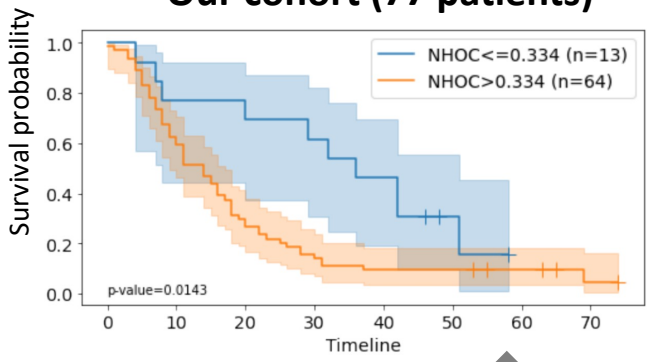


VALID

Large NHOC value
→ poor patient outcome

**[Jimenez-Sanchez et al.]**

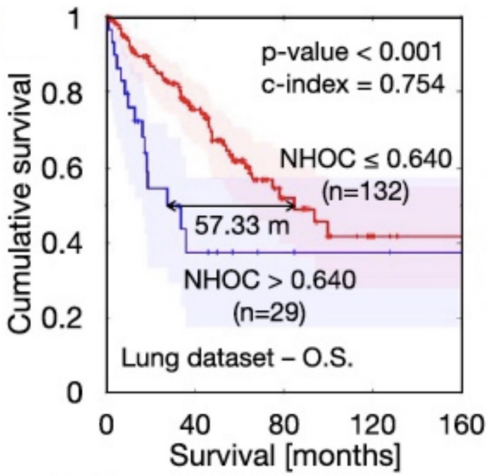


## Combination of prognostic PET biomarkers

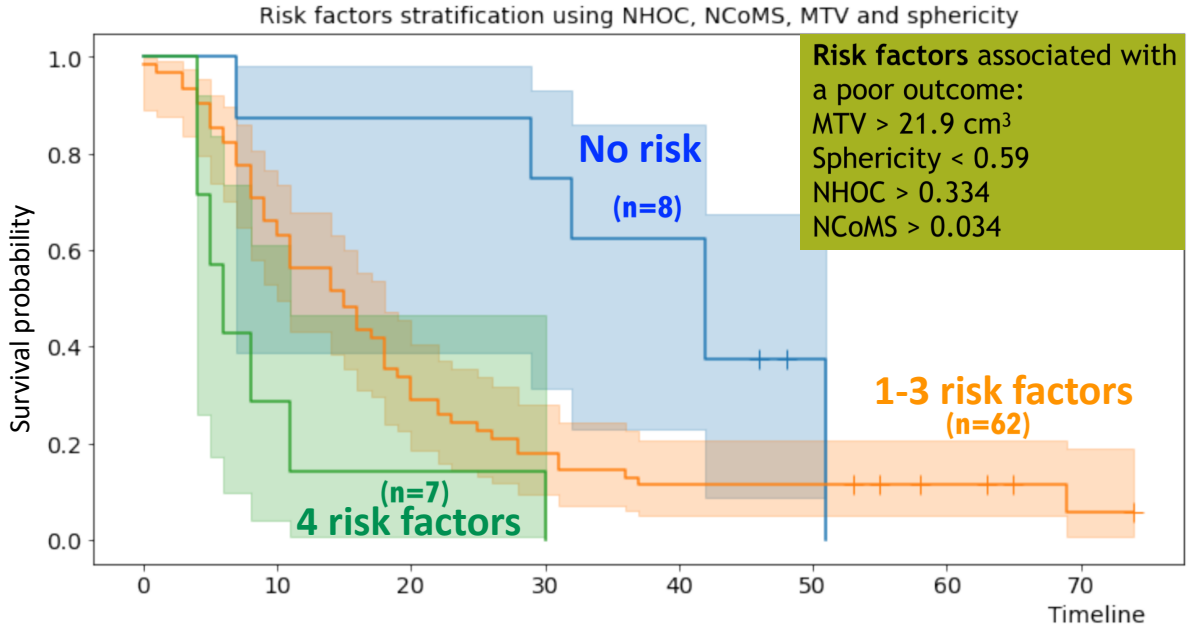


**<u>Independent validation</u> of the prognostic value of NHOC and combination of 4 PET-derived biomarkers to stratify lung cancer patients according to OS**


Thanks to all colleagues who sent me slides and answered my questions and apologies for scribbling on the slides!

Apologies to all who sent slides that I could not include for the sake of time